

HEAT TRANSFER TO WATER FLOWING IN AN ELECTRICALLY
HEATED HORIZONTAL TUBE

by

ROSS SIDDONS PHILIPS

Bachelor of Science

University of Oklahoma

Norman, Oklahoma

1950

Submitted to the faculty of the Graduate School of
the Oklahoma State University
in partial fulfillment of the requirements
for the degree of
MASTER OF SCIENCE
May, 1959

NOV 18 1959


HEAT TRANSFER TO WATER FLOWING IN AN ELECTRICALLY
HEATED HORIZONTAL TUBE

Thesis Approved:



Thesis Adviser





Dean of the Graduate School

PREFACE

The purpose of this thesis was to investigate the effect of flow rate and heat flux on the film coefficient during forced convection flow at various pressures. The results are compared with the established Colburn correlation. To familiarize the reader with the heat transfer loop used in the experimentation, a descriptive chapter is included.

I wish to thank Dr. J. H. Boggs for his capable direction of the research program. Appreciation is expressed to Mr. G. E. Tanger for his suggestions in the writing of this thesis. I am indebted to Professor B. S. Davenport and the personnel of the Mechanical Engineering Laboratory, without whose help the construction of the loop would not have been possible. Acknowledgement would be incomplete without mentioning the Boeing Airplane Company, whose graduate study scholarship enabled me to pursue an advanced degree.

TABLE OF CONTENTS

Chapter	Page
I. INTRODUCTION	1
II. SURVEY OF LITERATURE	4
III. DESCRIPTION OF TEST APPARATUS	6
Flow Description	6
Main Circulating Pump	13
Preheater	14
Test Section	14
Sight Glass	19
Exhaust Header	20
Condenser	20
Holdup Tank	20
Condensate Transfer Pump	21
Supply Tank	21
Ion Exchange System	21
Temperature Measurements	23
Pressure Measurements	23
Flow Measurements	26
Power Measurements	26
Safety Features	27
IV. CALIBRATION OF THERMOCOUPLES AND ORIFICE	28
Calibration of Thermocouples	28
Calibration of .353-inch Diameter Orifice Plate	34
V. EXPERIMENTAL PROCEDURE AND PRESENTATION OF DATA	39
Experimental Procedure	39
Presentation of Data	41
VI. ANALYSIS OF DATA	45
Method of Analysis	45
Sample Calculations	58
Discussion	60
VII. CONCLUSIONS	62
SELECTED BIBLIOGRAPHY	63
APPENDIX	64

LIST OF TABLES

Table	Page
I. Freezing Points of Metal Samples	28
II. Temperature Corrections Determined from Freezing of Metal Samples	29
III. Tabulation of Heat Transfer Data	43
IV. Results of Heat Transfer Analysis	53

LIST OF PLATES

Plate	Page
I. Overall View of Test Facility	7
II. View of Exhaust Manifold	8
III. View of Test Section	9
IV. Rear View of Manometer System	10

LIST OF ILLUSTRATIONS

Figure	Page
1. Schematic Diagram of Test Facility	11
2. Control Panel	12
3. Pump Performance	15
4. Preheater Construction	16
5. Test Section	18
6. Ion Exchange System	22
7. Pressure Measurement System	25
8. Cooling Curve for Tin Sample	30
9. Cooling Curve for Lead Sample	31
10. Cooling Curve for Zinc Sample	32
11. Temperature Correction Vs. Thermocouple Reading	33
12. Orifice Calibration Curve	37
13. Flow Rate Vs. In. Manometer	38
14. Film Coefficient, h_c , Vs. Bulk Temperature for Heating Water at Various Mass Flow Rates, G, Inside a Tube with a .400-inch I.D.	46
15. Voltage Drop Vs. Length for Run No. 11	48
16. Analysis Results for Run No. 153	61
17. Specific Heat Vs. Temperature Saturated Liquid Water	65
18. Prandtl Number Vs. Temperature Saturated Liquid Water	66
19. Dynamic Viscosity Vs. Temperature Saturated Liquid Water	67

Figure	Page
20. Thermal Conductivity Vs. Temperature for Saturated Liquid Water	68
21. Specific Volume Vs. Temperature Saturated Water	69
22. Saturation Temperature Vs. Saturation Pressure for Water	70
23. Thermal Conductivity of AISI Type 304 Stainless Steel.	71

SYMBOLS AND ABBREVIATIONS

A	= Surface area, ft ²
A _c	= Cross-sectional area of internal pipe diameter, ft ²
A _s	= Inside surface area of tube, ft ²
C	= Orifice coefficient of discharge, dimensionless
C _p	= Specific heat of fluid, Btu/lb F
\bar{C}_p	= Average specific heat, based on the average of the fluid temperature at the inlet and the bulk temperature of the fluid at the preceding evaluation point, Btu/lb F
D	= Inside diameter of tube, ft
D _e	= Equivalent diameter, equal to four times the hydraulic radius based on total perimeter, ft
G	= Mass flow rate, per unit area, lb/hr ft ²
g	= Acceleration of gravity, 32.17 ft/sec ²
h	= Heat transfer coefficient, Btu/hr ft ² F
h _c	= Film coefficient evaluated from Colburn equation, Btu/hr ft ² F
h _i	= Film coefficient at point i, Btu/hr ft ² F
h _l	= Differential head across orifice, in feet of flowing fluid
K	= Thermal conductivity, Btu/hr F ft
K _f	= Thermal conductivity of fluid evaluated at the film temperature, Btu/hr F ft
K ₁₂	= Thermal conductivity of the first layer of insulation, Btu/hr F ft

- K_{23} = Thermal conductivity of the second layer of insulation,
 Btu/hr F ft
- L = Total length of the test section, in.
- l_i = Length measured from inlet power terminal to the point where
 the film coefficient is evaluated, in.
- p = Total power input to the test section, kw
- q = Heat flow per unit time, Btu/hr
- q' = Heat flow, Btu/hr ft
- q'' = Heat flow per unit time per unit area, Btu/hr ft²
- Re = Reynolds number, dimensionless
- r_i = Inside radius of tube, in.
- r_o = Outside radius of tube, in.
- r_1 = Radius of pipe, ft
- r_2 = Radius of first layer of insulation, ft
- r_3 = Radius of second layer of insulation, ft
- t_b = Bulk temperature of fluid, F
- t_{b_i} = Bulk temperature of fluid at point where the film coefficient
 is evaluated, F
- Δt_{b_i} = Bulk temperature rise of fluid from inlet to point where
 the film coefficient is evaluated, F
- t_e = Bulk temperature of fluid at inlet of test section, F
- Δt_f = Temperature difference between the surface and the fluid, F
- Δt_{f_i} = Film temperature drop at the point where the film coefficient
 is evaluated, F
- t_s = Surface temperature, F
- t_{s_i} = Inside temperature of the tube at the point where the film
 coefficient is evaluated, F

- t_{wi} = Outside surface temperature at the point where the film coefficient is evaluated, F
- Δt_{wi} = Temperature drop through wall at the point where the film is evaluated, F
- t_1 = Wall temperature, F
- t_3 = Outside surface temperature, F
- V_1 = Volume rate of flow, ft³/sec
- W = Flow rate, lb/min
- μ = Dynamic viscosity of fluid, lb/hr ft
- μ_f = Dynamic viscosity of fluid evaluated at the film temperature, lb/hr ft
- μ_w = Dynamic viscosity of fluid evaluated at the wall temperature, lb/hr ft

CHAPTER I

INTRODUCTION

The heat transfer loop constructed in the Mechanical Engineering Laboratory at Oklahoma State University can furnish heat transfer and pressure drop information for fluids in the regions of forced convection, local boiling, and two phase flow. Of these three types of convective heat transfer which the loop is capable of producing, forced convection is most commonly used. As the effects of local boiling and two phase flow become better known, it is possible that there will be applications such as nuclear reactors, which will incorporate a phase change of the coolant. Though more is known about forced convection, most calculations are made with empirical equations based on correlations of experimental data. The purpose of this thesis is to investigate the effect of flow rate and heat flux at various pressures on the film coefficient during forced convection flow, and compare the results with the established Colburn correlation.

Newton introduced the concept of a heat transfer, or so-called "film" coefficient, and recommended the following equation for heat transfer during convection:

$$q = h A \Delta t_f$$

where

q = heat flow per unit time, btu/hr

h = heat transfer coefficient or film coefficient, Btu/hr ft²F

A = surface area, ft²

Δt_f = temperature difference between the surface and the fluid, F.

This equation is sometimes called Newton's Law of Cooling, but is really a definition of h instead of a law. It states that the heat transfer per unit area, and time from a surface to a fluid flowing along it, is equal to the product of the temperature difference between the surface and a quantity, h , which depends on the convection character of the flowing fluid.

Newton's equation can be arranged as follows:

$$q/A = q'' = h \Delta t_f$$

where

q'' = heat flow per unit time per unit area, Btu/hr ft²

If the heat flux, film coefficient, and fluid temperature are known at a point, the surface temperature can be determined from

$$t_{\text{surface}} = t_{\text{bulk}} + \Delta t_f$$

The object of the heat transfer experiment was to determine "h" for the conditions of forced convection in an electrically heated horizontal tube. The tube was .500 inch O. D. with a .050 inch wall, and was 7 feet long. The tube was made of type 304 stainless steel. The outside surface temperature was measured along the length of the tube; the inside surface temperature was calculated. The change in bulk temperature of the fluid with length was determined using a heat balance.

With the variation with length of the inside surface and fluid

temperatures known, a point determination of "h" was possible by applying the equations

$$\Delta t_f = t_s - t_b$$

and

$$h = q'' / \Delta t_f.$$

The calculated value of the film coefficient was compared with film coefficients evaluated from existing correlations. The film coefficient during forced convection has been correlated by Colburn (1), for any fluid with a Prandtl number greater than .7 in turbulent flow, and is expressed by dimensionless numbers in the equation

$$\frac{hD}{K} = 0.023 \left[\frac{GD}{\mu} \right]^{0.8} \left[\frac{\mu C_p}{K} \right]^n$$

where

n = 0.3 when the fluid is cooled

n = 0.4 when the fluid is heated.

CHAPTER II

SURVEY OF LITERATURE

For turbulent flow heat transfer without change of phase inside tubes or in annuli, the following equations are most widely used:

Dittus and Boelter (2) correlated heat transfer data for heating liquids, and found that the following equation expressed their results:

$$\frac{hD}{K} = 0.0265 \left[\frac{DG}{\mu} \right]^{0.8} \left[\frac{C_p \mu}{K} \right]^{0.4} \quad (1)$$

Colburn (1) correlated heat transfer data for heating or cooling liquids in tubes with the following equation:

$$\frac{hD}{K} = 0.023 \left[\frac{DG}{\mu} \right]^{0.8} \left[\frac{C_p \mu}{K} \right]^n \quad (2)$$

Sieder and Tate (3) correlated heat transfer data for heating or cooling liquids in tubes, and found that the following equation expressed their results:

$$\frac{hD}{K} = 0.027 \left[\frac{DG}{\mu} \right]^{0.8} \left[\frac{C_p \mu}{K} \right]^{1/3} \left[\frac{\mu}{\mu_w} \right]^{0.14} \quad (3)$$

Carpender, Colburn, Schoenborn, and Wurster, (4) correlated heat transfer data for heating liquid in an annulus with the following equation:

$$\frac{hD_e}{K} = 0.023 \left[\frac{DG}{\mu} \right]^{0.8} \left[\frac{C_p \mu}{K} \right]^{1/3} \left[\frac{\mu}{\mu_w} \right]^{0.14} \quad (4)$$

For annuli, the equivalent diameter is taken as four times the hydraulic radius, based on total wetted perimeter. At the moderate values of Δt , ordinarily used with heat transfer to water, all these equations predict nearly the same values of the heat transfer coefficient.

CHAPTER III

DESCRIPTION OF TEST APPARATUS

Flow Description

The water heat transfer loop shown in Plates I, II, III, and IV, circulated high resistivity distilled water inside a horizontal, tubular test section. The test section was heated electrically, and the circulated water was heated by the tube. System pressure was controlled by throttling the flow at the terminal end of the loop.

Figure 1 is a schematic flow diagram of the heat transfer loop. Water was pumped from the supply tank by the main circulating pump. The bulk temperature of the water leaving the pump was measured by the use of a thermocouple. Water leaving the pump flowed through one of two orifices and through a bypass valve to the holdup tank to be returned to the supply tank. This bypass line includes a valve mounted on the control panel, Fig. 2, so that minor adjustments can be made in the flow rate. The orifice pressure taps are connected to a differential pressure transmitter and to a manometer in parallel with the transmitter. The differential pressure transmitter, the air actuated control valve, and the flow controller mounted on the control panel were not used at any time during the experiment as it was found that the main circulating pump maintained a uniform flow rate.

Upon passing through the selected orifice, the water entered the

PLATE I

OVERALL VIEW OF TEST FACILITY

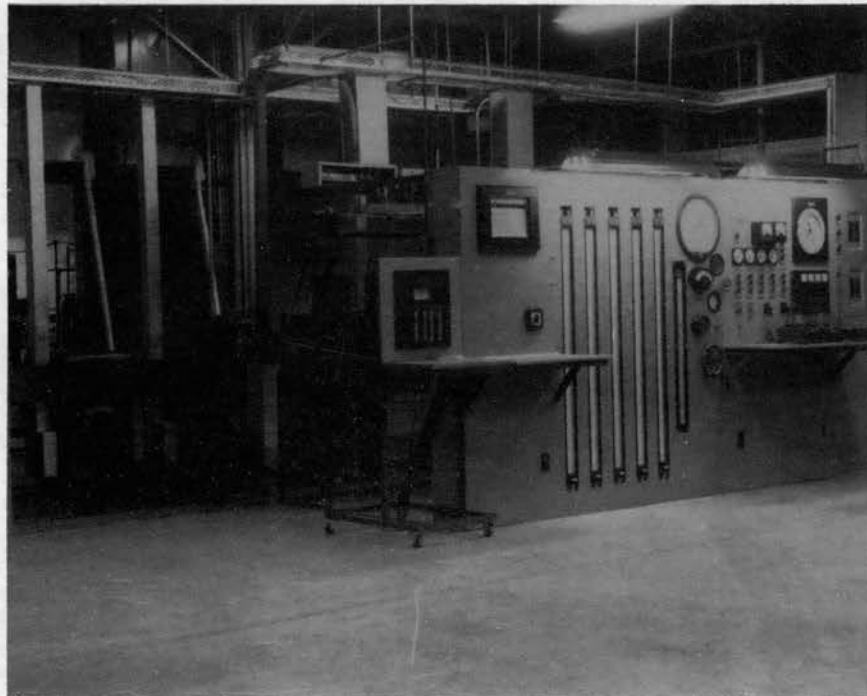


PLATE II

VIEW OF EXHAUST MANIFOLD

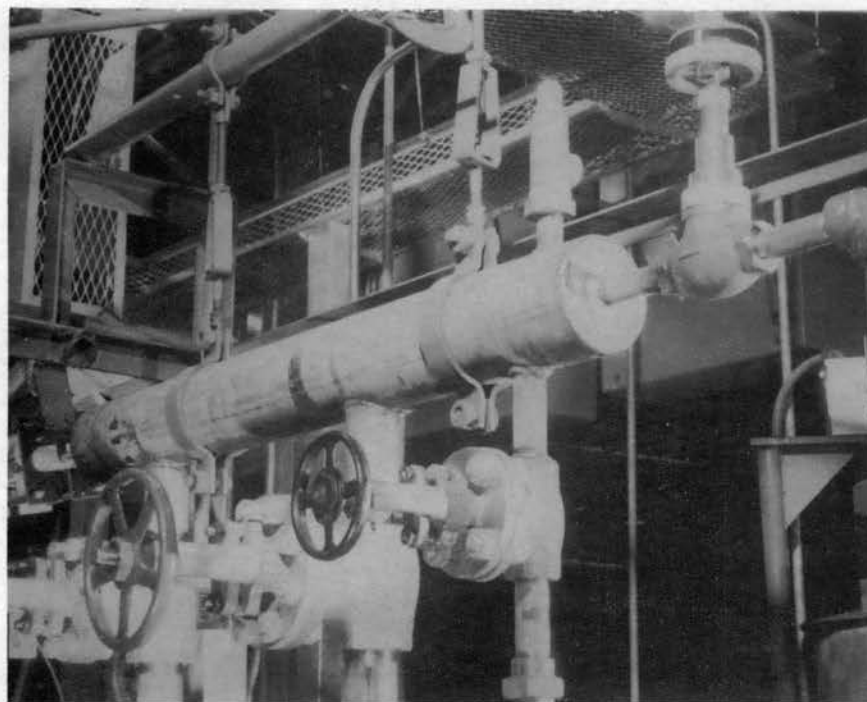


PLATE III

REAR VIEW OF MANOMETER SYSTEM

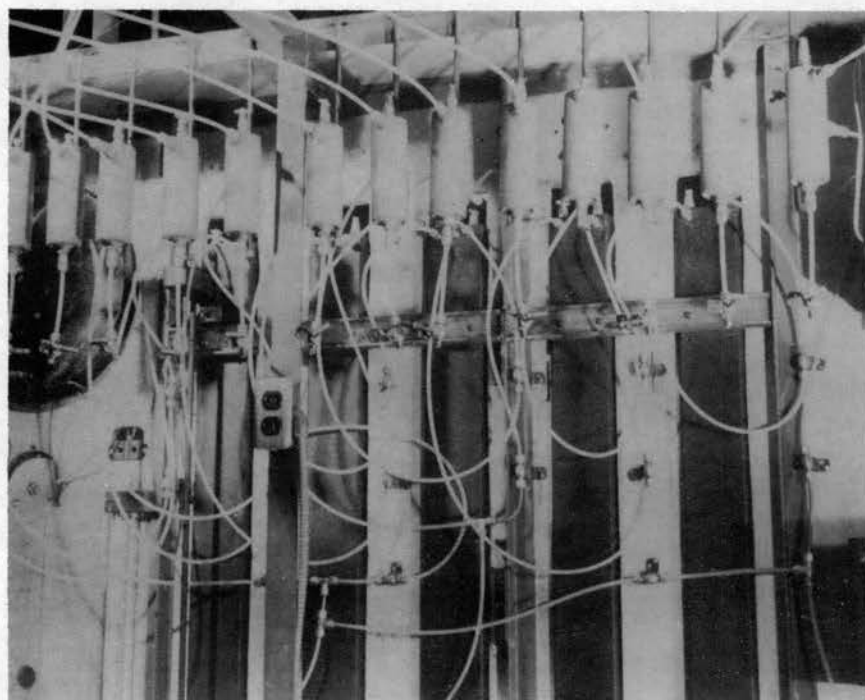
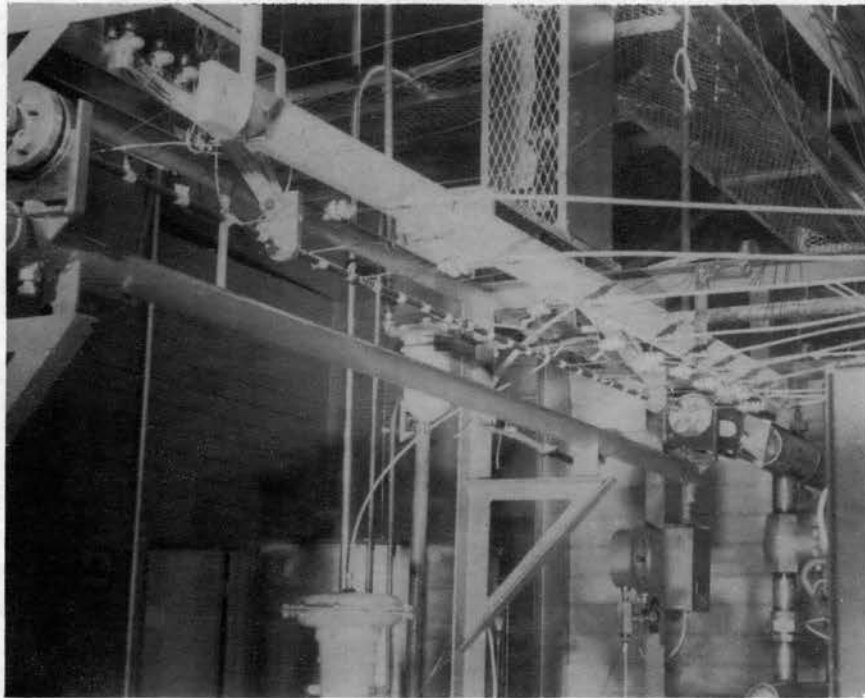


PLATE IV
VIEW OF TEST SECTION



STRATHMORE PARCHMENT

100% RAG U.S.A.

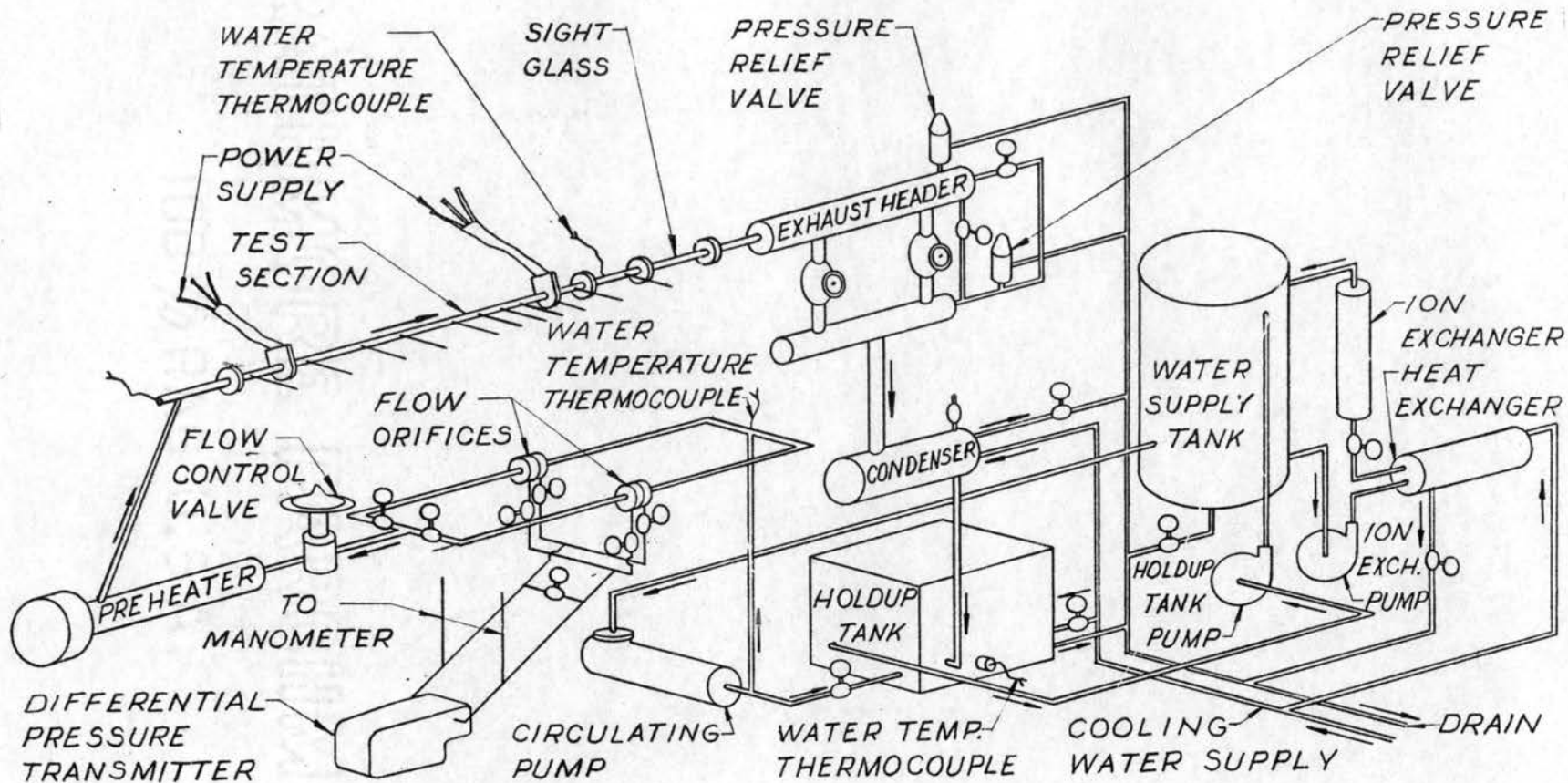
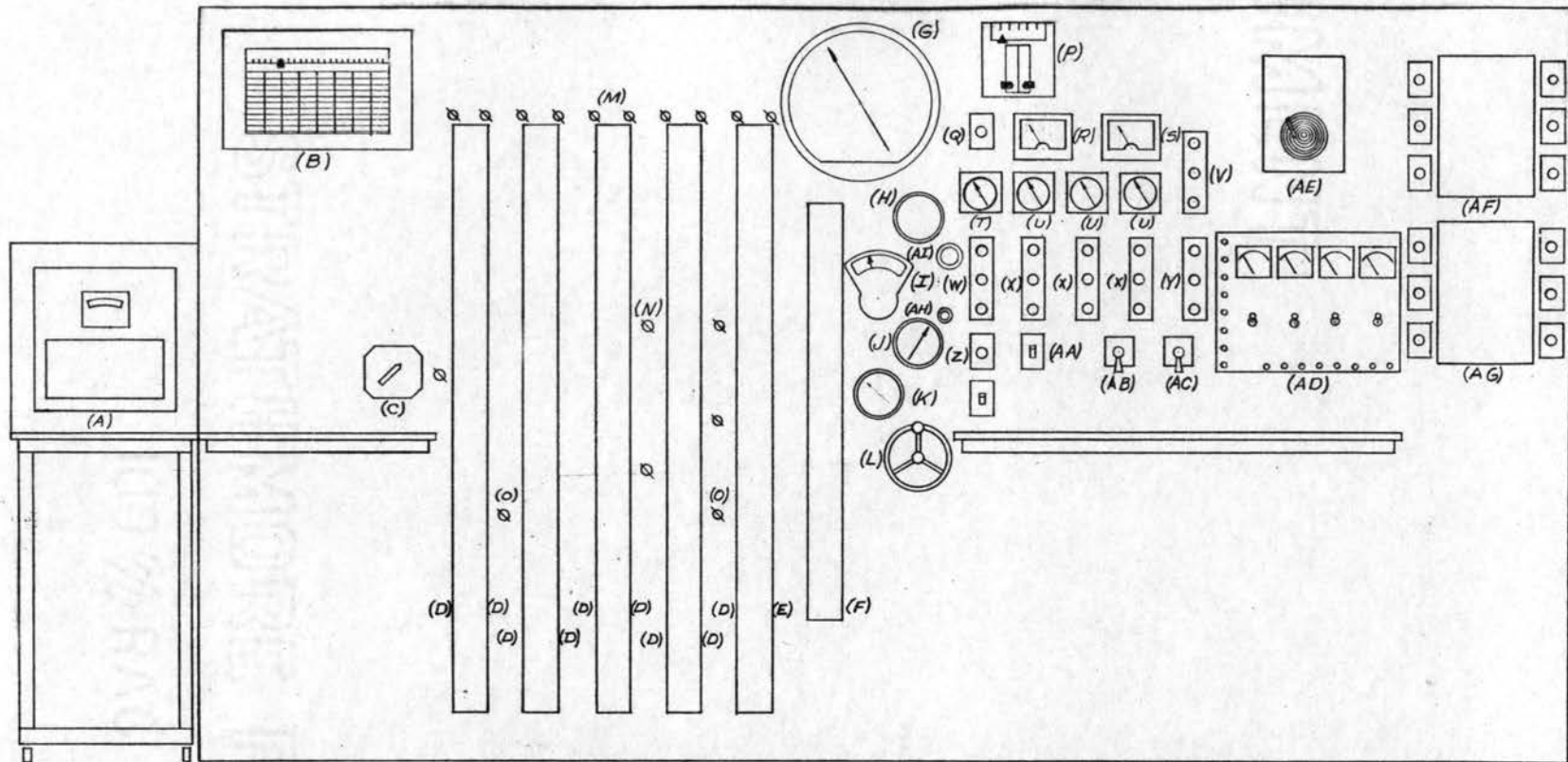


FIGURE 1
SCHEMATIC DIAGRAM
OF TEST FACILITY



- (A) 48 POINT TEMPERATURE INDICATOR
- (B) TEMPERATURE RECORDER
- (C) THERMOCOUPLE SELECTOR SWITCH
- (D) PRESSURE DROP MANOMETERS
- (E) FLOW MANOMETER
- (F) 36 INCH MANOMETER
- (G) PRECISION PRESSURE GAGE
- (H) OBSERVATION PORT
- (I) VARIDRIVE SPEED INDICATOR
- (J) SYSTEM PRESSURE
- (K) HOLDUP TANK TEMPERATURE INDICATOR
- (L) VARIDRIVE SPEED ADJUSTMENT
- (M) MANOMETER VALVES

- (N) MANOMETER BYPASS VALVES
- (O) MANOMETER REFERENCE VALVES
- (P) CONTROL SYSTEM PRESSURE INDICATOR
- (Q) PANIC SWITCH
- (R) TEST SECTION VOLTMETER
- (S) TEST SECTION WATTMETER
- (T) TOTAL CURRENT AMMETER
- (U) INDIVIDUAL TRANSFORMER AMMETER
- (V) DIRECT CONNECTED PREHEATER
- (W) MAIN PUMP SWITCH
- (X) TRANSFORMER POWER SWITCH
- (Y) POWERSTAT SWITCH
- (Z) TRANSFER PUMP SWITCH

- (AA) ION PUMP SWITCH
- (AB) POWER TRANSFORMER DRIVE SWITCH
- (AC) POWERSTAT POSITION SWITCH
- (AD) PREHEATER INSTRUMENT PANEL
- (AE) TEST SECTION CURRENT RECORDER
- (AF) PREHEATER JUNCTION BOX
- (AG) POWERSTAT JUNCTION BOX
- (AH) BYPASS VALVE
- (AI) THROTTLE VALVE

FIGURE 2
CONTROL PANEL

preheater. Preheat power is partially controlled by a Powerstat that is adjusted remotely from the control panel. The bulk temperature of the water was measured before entering the test section, and was again measured upon leaving the heated portion of the test section. Electrical power is introduced to the test section through copper lugs and is supplied by three welding transformers connected in parallel. The transformers are adjusted remotely from the control panel. Static pressure taps and outside wall temperature thermocouples are located at numerous positions along the test section. A sight glass installed at the outlet of the test section allowed observation of the flow leaving the test section.

The fluid then entered the exhaust header and was throttled down to atmospheric pressure. All steam was condensed to saturated water at this point. The fluid then entered the water cooled heat exchanger where it was cooled. The fluid leaving the heat exchanger entered the holdup tank and was cooled further. Condensate was returned to the supply tank by a transfer pump which operated intermittently. The pump is controlled by a float in the supply tank.

Water in the supply tank was circulated through an ion exchange system using a pump. The water was forced through a water cooled heat exchanger where it was cooled. Leaving the heat exchanger, the system water was forced up through the vertical ion exchanger and returned to the supply tank.

Main Circulating Pump

To insure that the pressure drop experienced by the fluid in the test section did not influence the rate of flow of the pump, a pump having a flat capacity versus head curve was chosen. The characteristic

curves of this pump are shown in Fig. 3. The pump is a Moyno progressing-cavity type manufactured by Robbins and Myers, Inc. The pulley diameter of the pump is 8.6-inches and its speed range is from 215 to 2900 RPM, although the recommended operating range is from 300 to 1750 RPM.

The main circulating pump is driven by a U. S. Varidrive Syncrogear Motor having a speed range of 366 to 5000 RPM, and a pulley diameter of 5-inches. The speed of the varidrive is remotely controlled from the control panel by a bevel gear and rod linkage. A tachometer on the varidrive is connected to an indicator on the control panel.

A stainless steel flexible connection is installed in the line immediately downstream of the pump to prevent vibrations of the pump and its drive from being transmitted to the test section structure.

Preheater

Twelve immersion heaters are installed in a 5-inch schedule 40 stainless steel enclosure, as shown in Fig. 4. These Chromalox, MT-201, heater elements have a rating of 5000 watts each at 240 VAC. Six of these elements are connected directly to line voltage through appropriate switches. The six remaining switches are connected through individual switches to a variable transformer (Powerstat) with a remote control drive. Thus it is possible to deliver any increment of the 45 kw of available power to the preheater by using any number of the six directly connected heater elements and controlling the Powerstat output.

Test Section

The test section was constructed from a round, type 304, stainless steel tube, having an inside diameter of .400-inch and a wall thickness

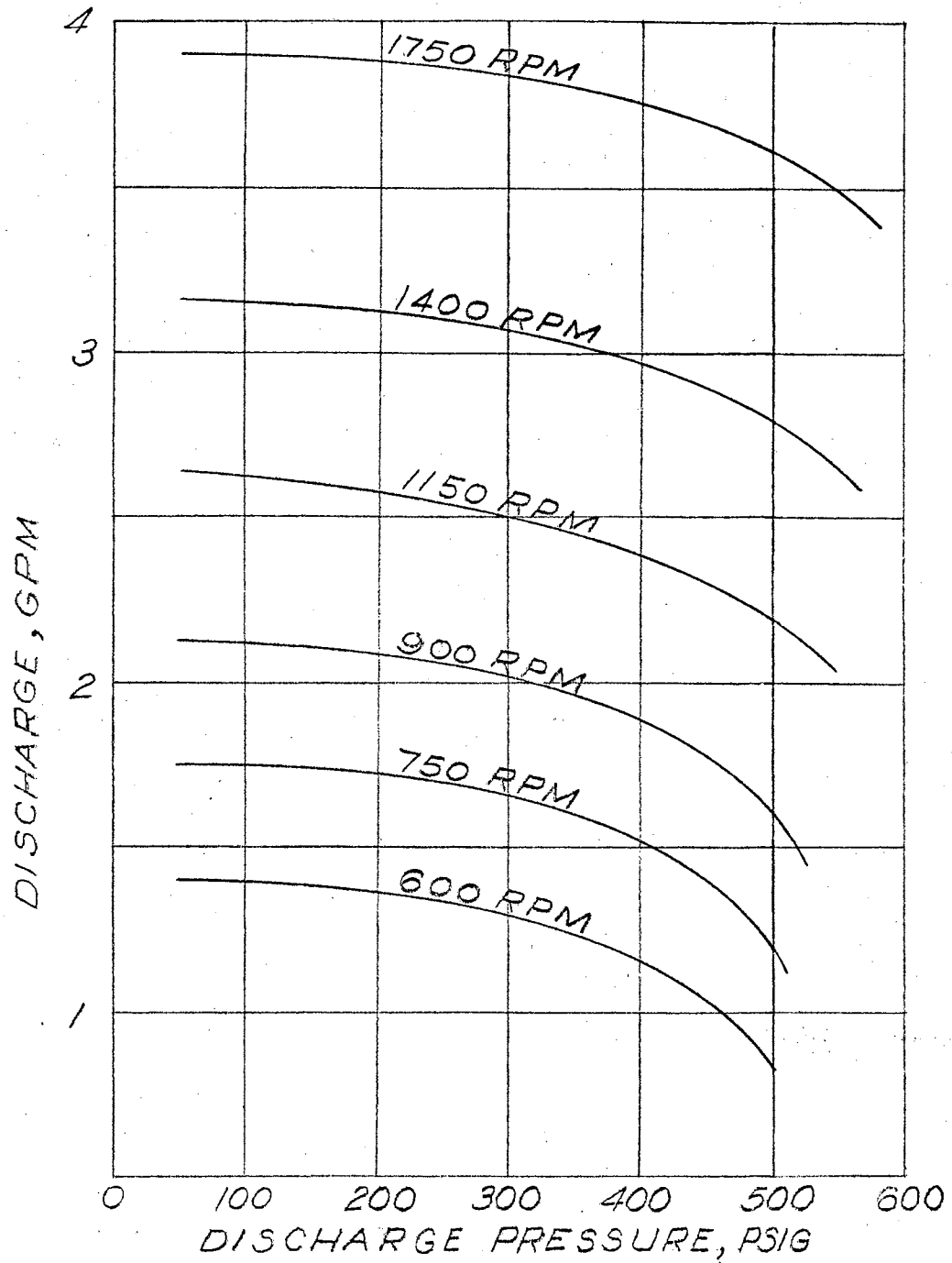


FIGURE 3
PUMP PERFORMANCE
FOR 6 STAGE MOYNO PUMP

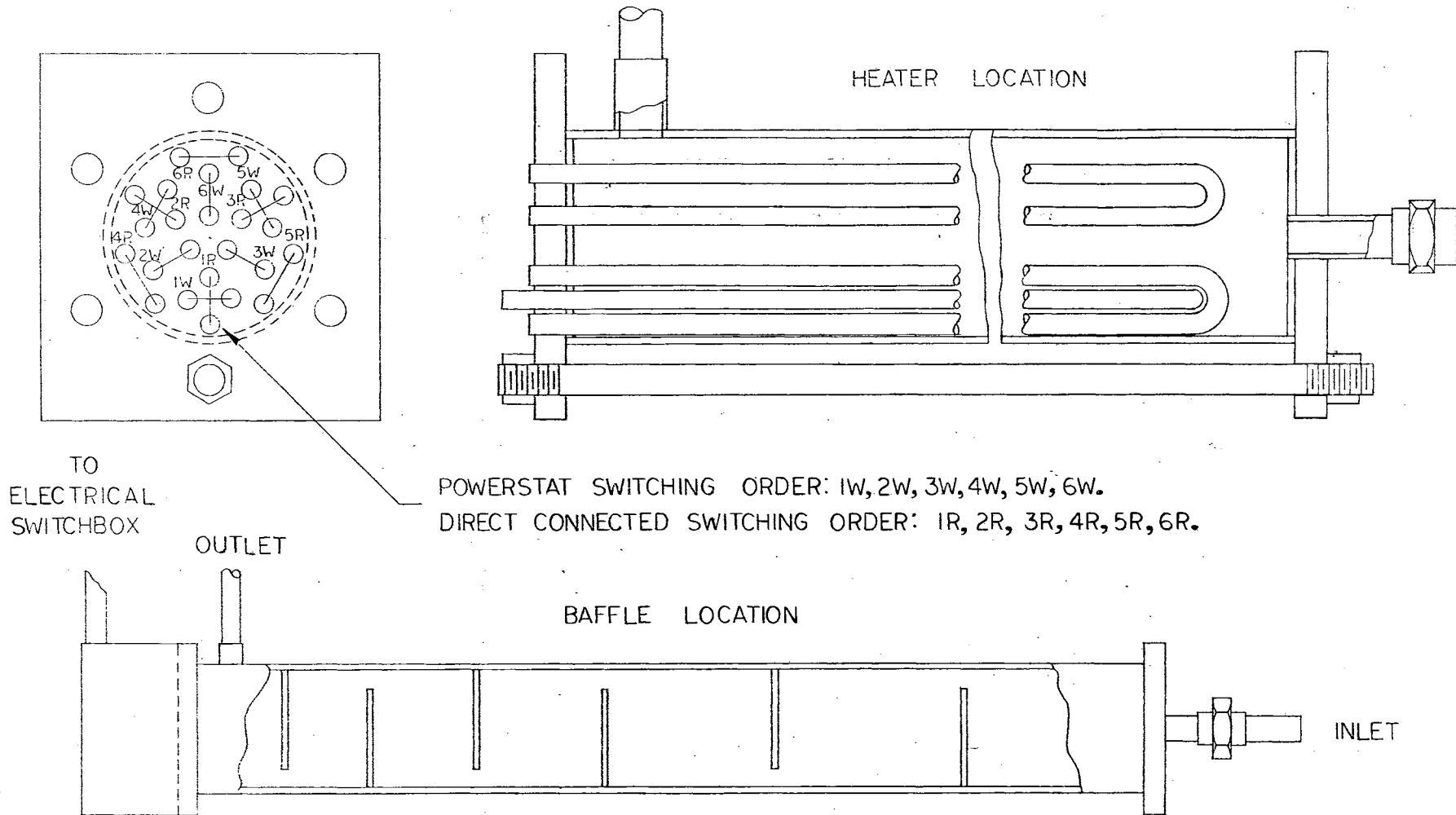
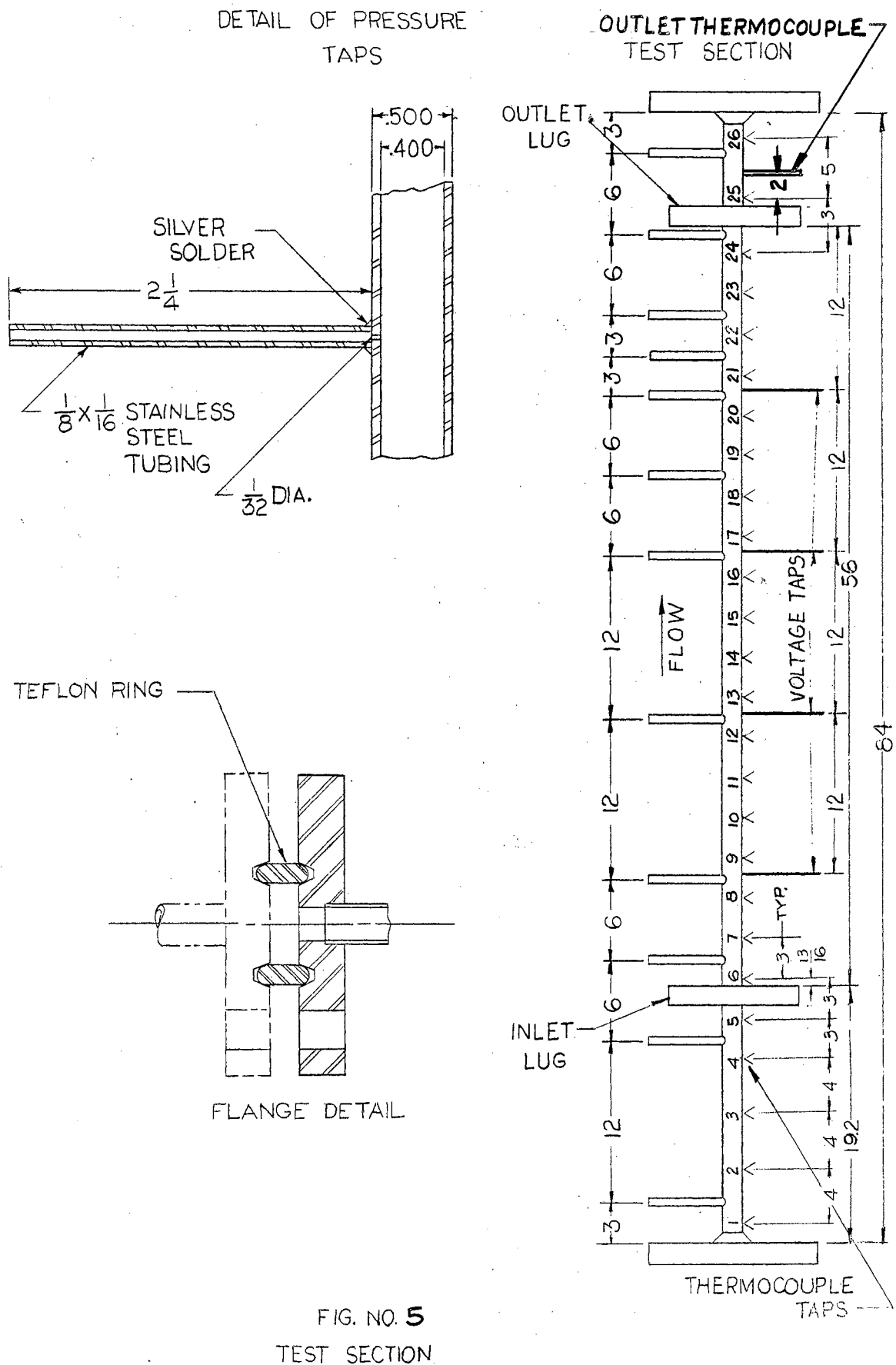


FIGURE 4
 PREHEATER CONSTRUCTION

of .050-inch. As shown in Fig. 5, the overall length of the tube was 7 feet.

A flexible stainless steel connection is installed in the pipe between the preheater and the test section entrance to allow for the thermal expansion of the test section. Power was applied to the tube across the copper terminals that were silver soldered to the tube. The connecting flanges at either end of the test section are fitted with teflon insulators to prevent current from passing through the piping to other parts of the system. Single phase, alternating current is supplied to the test section from three Lincoln 400 "Fleetwelder Special" 20 kw welding transformers. The transformers are rated at 113 amperes input at 220 volts and a Nema rating of 400 amperes output at 40 volts. The power output of the transformers is changed in a stepless manner by adjusting a positioning switch on the control panel, Fig. 2. This switch actuates an electric motor which simultaneously adjusts a rotary voltage induction regulator on each transformer by means of a chain drive. Switches on the control panel, Fig. 2, allow selection of any combination of the three transformers; however, those selected shared the load equally because of the positioning scheme described above.

Ten pressure taps were silver soldered to the surface of the tube positioned as shown on Fig. 5. They were constructed of type 304, stainless steel tubing, 1/8-inch O. D., 1/16-inch I. D., and 2 1/4-inch in length. A 1/32-inch diameter hole was drilled radially in the tubing. Burrs produced by the drilling operation were removed so that a smooth inside surface resulted. Each of the pressure taps was fitted with line coolers made from copper tubing wound into a helical coil. Cotton was stuffed into the coil and wetted at various intervals during testing



to prevent damage to the nylon tubing used for pressure drop measurements.

A thermocouple was installed in the test section to measure the exit temperature of the fluid. Its position is shown in Fig. 5. Twenty six thermocouples were spot welded to the outside surface of the tube in the positions indicated on Fig. 5. These junctions were wrapped with glass tape.

Four voltage taps were soldered at equal intervals along the length of the test section as shown in Fig. 5. Voltage taps were also located on each of the terminals supplying power to the test section. Thus voltage measurements could be made in five increments along the length of the heated portion of the tube between the power terminals.

Plate III is a photograph of the test section showing the thermocouples, pressure taps and voltage taps installed.

After installation of the thermocouples, pressure taps, and voltage taps, the test section was carefully wrapped with a layer of 1/16-inch thick asbestos. Glass wool insulation was then wrapped over the asbestos to an approximate outside diameter of 3 3/4-inch. Finally, aluminum foil was wrapped over the glass wool to complete the insulation of the test section. Four 30 gauge (.010-inch wire diameter) iron constantin thermocouples were inserted in the insulation at various depths to check the heat loss through the insulation.

Sight Glass

A pyrex glass, with the same inside diameter as the test section is installed in the system immediately downstream of the test section in order that flow phenomena can be observed. The glass tube is fitted with teflon seals on either end to prevent fluid leakage. By observing the

fluid in the glass tube through the observation port in the control panel, Fig. 2, the occurrence of boiling at the tube exit can be determined.

Exhaust Header

The exhaust header is constructed of a horizontal 4 1/2-inch stainless steel pipe and a horizontal 3-inch stainless steel pipe connected by two 2-inch gate valves, a 1-inch globe valve, and a 1/2-inch needle valve. The gate and globe valves are used for large adjustments in pressure, and the 1/2-inch needle valve is used for small adjustments in pressure. The 1/2-inch needle valve is positioned remotely with a handwheel on the control panel, Fig. 2. The exhaust header is fitted with a 550 psi safety valve. Thus if system pressure exceeds 550 psi, the valve opens and protects the equipment of the system. Plate II is a photograph of the exhaust header.

Condenser

A Ross, type BCF, 501-2, two pass heat exchanger, with admiralty tubes and brass body, is used to cool the condensate leaving the exhaust header. An air vent is attached to the condenser for the purpose of removing entrained air in the system fluid.

Holdup Tank

The final cooling of the system fluid occurs in the holdup tank. The holdup tank is constructed of welded stainless steel sheet. Two separate copper coils are installed in the tank. The copper coils are attached to headers, and a valving arrangement allows use of one or both of the cooling coils. System fluid is allowed to stand in the tank for

a period of time determined by the float valve setting in the supply tank that regulates the operation of the condensate transfer pump. A gas thermometer is installed in the tank and the temperature of the water is indicated on a gauge on the control panel, Fig. 2.

Condensate Transfer Pump

A Yeoman Bros. pump, having a 1-inch suction port and a 3/4-inch discharge port, driven by a 1/3 hp, single phase, 115 volt totally enclosed General Electric motor is used to transfer system fluid from the holdup tank to the supply tank. A float valve controls the level of water in the supply tank by intermittently switching electrical power to the pump motor.

Supply Tank

The supply tank is constructed of stainless steel, and its capacity is 100 gallons of water. A sight gauge is attached to the side of the tank in order that the level of the water in the tank can be determined conveniently.

Ion Exchange System

A schematic flow diagram of the ion exchange system is shown on Fig. 6. The ion exchange system is necessary for removal of contaminants from the water in order that the inside surface of the test section can be kept clean.

The pump used in this system is the same type as that used for condensate transfer.

The heat exchanger is constructed from a 4-inch O.D. steel pipe and approximately 20 turns of 1/4-inch copper tubing.

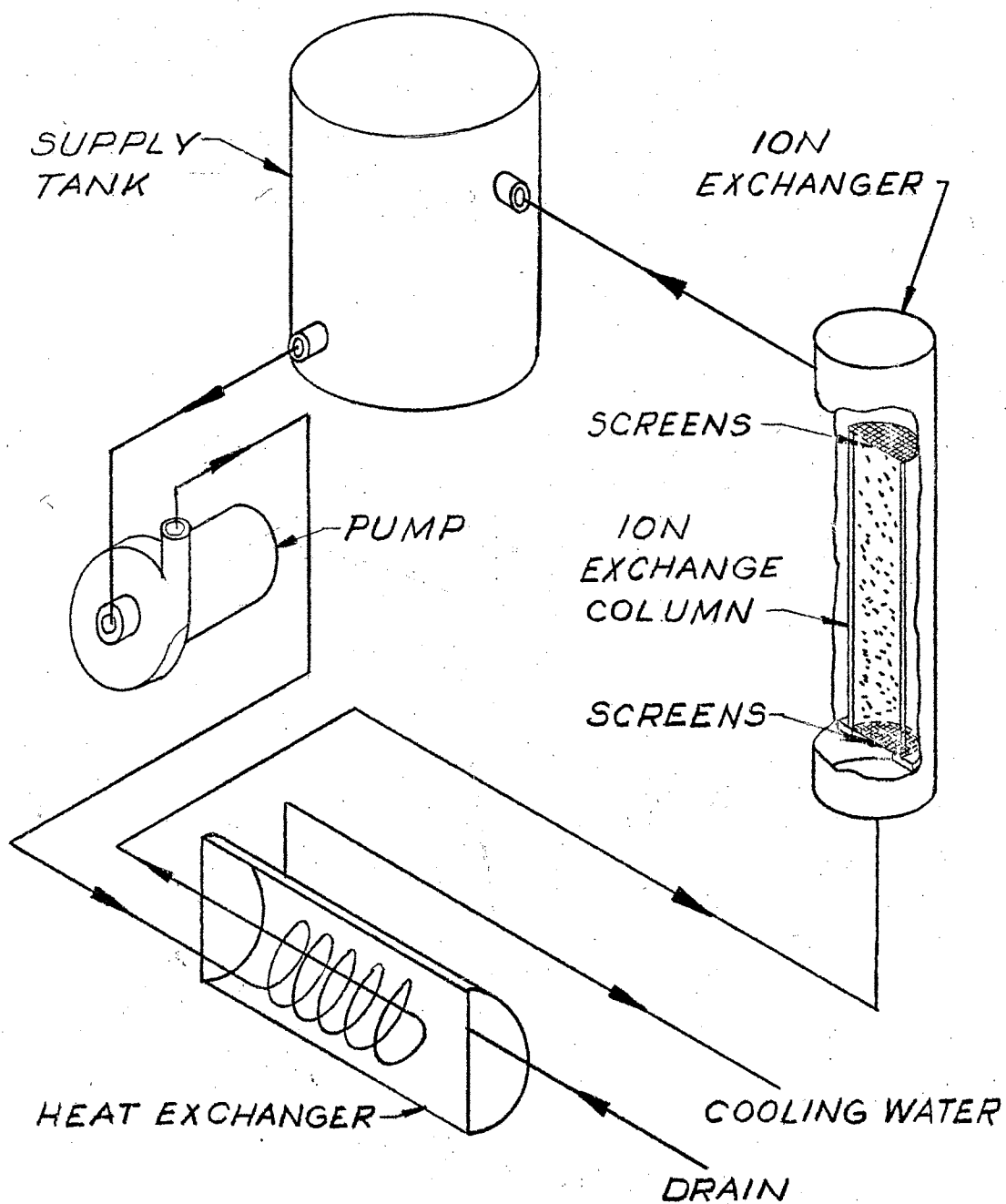


FIGURE 6
ION EXCHANGE SYSTEM

System water flowing inside the copper tubes is cooled by tap water flowing inside the pipe discharging to drain. By the use of this heat exchanger, water entering the ion exchanger column was kept below 100 F.

The ion exchanger column is constructed of stainless steel and has a capsule design which permits easy recharging of the resin used for the ion exchange media.

Temperature Measurements

All of the thermocouples used in the experiment were 30 gauge (.010-inch wire diameter) iron constantin thermocouples. The twenty six thermocouples attached to the test section, Fig. 5, the four thermocouples inserted in the test section insulation, the orifice inlet thermocouple, the test section inlet thermocouple, and the test section outlet thermocouple were all attached to the terminals of a Brown, type J, 48 point indicator. The indicator measured directly in degrees Fahrenheit, and had a range of 0 to 1200 F.

In addition, test section thermocouples 4, 6, 8, 10, 12, 14, 16, 18, 21, and 24, Fig. 5, attached to the indicator, were also connected to a Brown Electronik, type J, 10 point chart recorder with a range of 0 to 600 F. (The recorder was used to establish when the test section temperatures had reached a state of equilibrium.) Reading of temperature on the 48 point indicator was not recorded until equilibrium was reached.

The calibration of the thermocouples is discussed in Chapter IV.

Pressure Measurements

The upstream pressure tap attached to the test section was connected to the wells (or high pressure sides) of the nine Meriam, Series 30,

well-type manometers used to measure pressure differential along the length of the test section. The remaining nine pressure taps were connected to the low pressure side of the manometers. These connections are shown on Fig. 7. Plate IV is a photograph of the rear view of the manometer system. The manometers can withstand a maximum pressure of 500 psi. These manometers have a 60-inch scale, graduated in inches and tenths and were filled with Meriam Number 3 red fluid having a specific gravity of 2.95. The last well-type manometer in the fifth bank of manometers was used for determination of the pressure drop across the flow measurement orifices, as shown on the control panel, Fig. 2. The piping arrangement for the manometers was such that either all pressures could be measured in relation to the first pressure tap, as described above, or the pressures after tap number four could be measured in relation to number four.

A 0 to 750 psi precision Heise pressure gauge, 16-inches in diameter, mounted on the control panel, Fig. 2, was connected so that the static pressure at either pressure taps 1 or 9 could be measured. The Heise pressure gauge is accurate to plus or minus $1/4$ psi. An Acra pressure gauge was installed in parallel with the Heise gauge. Thus system pressure could be determined with the Acra gauge before the Heise was connected to the system.

The test section was electrically insulated from the pressure manometers by connecting nylon tubing.

Seal pots were located in the pressure sensing lines between the manometers and the test section to prevent red fluid from inadvertently entering the test section.

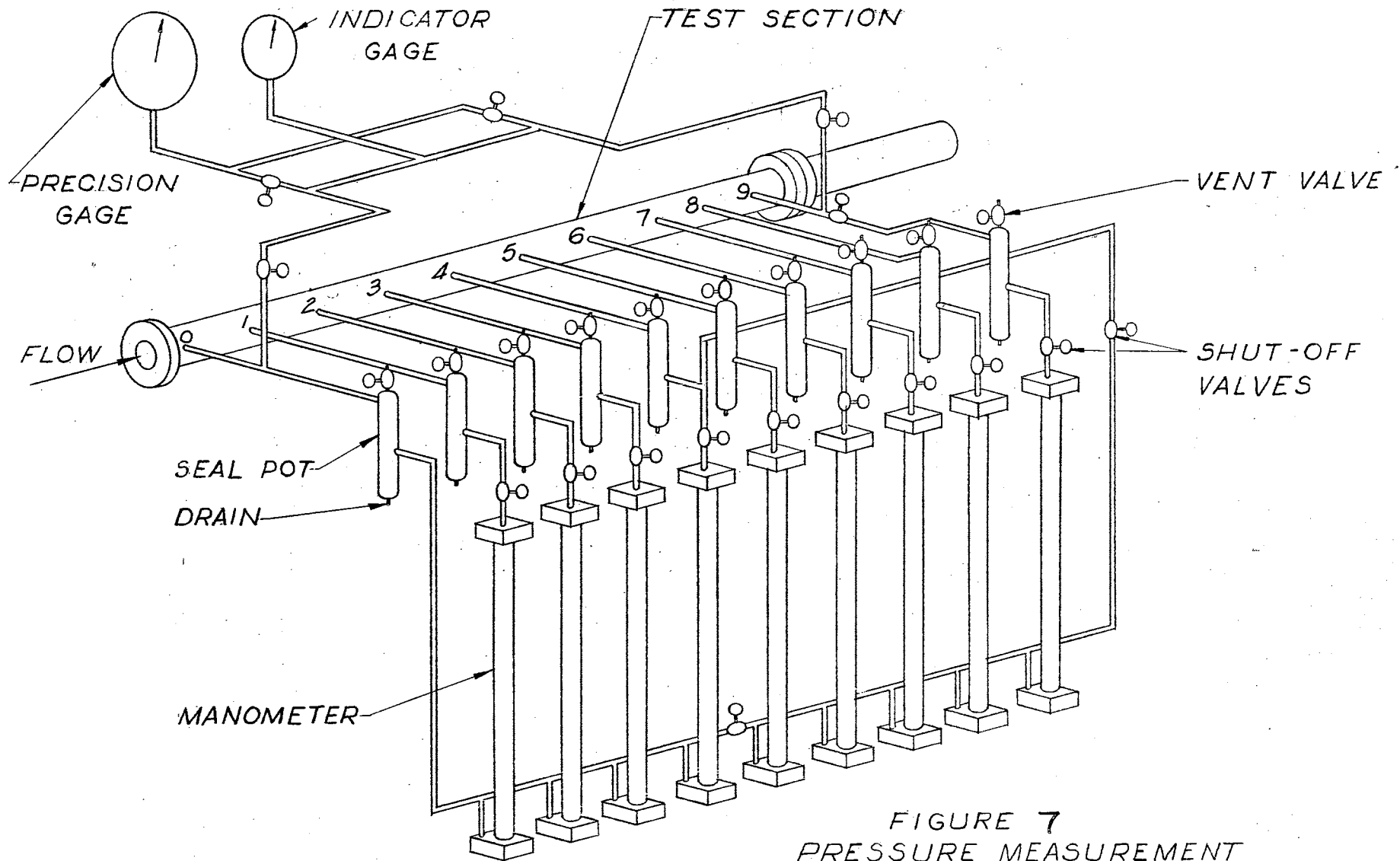


FIGURE 7
PRESSURE MEASUREMENT
SYSTEM

Flow Measurement

Two calibrated sharp edged orifices, 0.353-inch and 0.453-inch, are installed in parallel, Fig. 1, to measure the flow rate through the test section. Valves are installed in the parallel lines in order that the flow can be directed through either of the orifices. Gate valves are also provided in order that the pressure differential across either orifice can be measured by the manometer on the control panel, Fig. 2.

These orifices were supplied by the Daniel Orifice Fitting Co. and the calibration of the 0.353-inch orifice is outlined in Chapter IV. The 0.453-inch orifice was not calibrated as it was not used during these experiments.

Power Measurements

The total current through the test section is indicated by a 0 to 5 ampere General Electric Type AB Switch Board ammeter that receives current from a 300 to 1 General Electric instrument transformer. This ammeter is located on the control panel, Fig. 2. The six voltage taps connected to the test section were wired to jacks on the control panel in order that the voltage drops along the length of the test section could be measured conveniently. These voltage drops were measured with a General Electric Type P-3 voltmeter.

The current and voltage measurements for the preheater Powerstat and direct connected sections were made with precision Weston Model 155 AC portable instruments. Wiring connected to the appropriate points is connected to jacks on the control panel as shown on Fig. 2. Voltage is read directly, but the ammeters are connected through a 40 to 1 step

down instrument transformer.

A General Electric Type P-3 wattmeter is used to read test section power. Because of the method of connection it is necessary to multiply the wattmeter reading by 300. In the event the wattmeter's own range doubler is used, it is necessary to multiply the reading by 600.

A Brown Elektronik circular current recorder records the current through the test section in terms of percent of full scale deflection. The full scale deflection of the current recorder is 1500 amperes.

Safety Features

The water heat transfer loop includes several safety features which are required because of the hazard of applying power to a system that under some circumstances is not able to absorb it.

A General Electric automatic adjustable pressure switch is installed on the inlet cooling water line. The switch was set at approximately 30 psi so that all power to the preheater and the test section was cut off automatically if the cooling water pressure decreased below this value.

A Murphy pressure switch, adjustable between 0 and 600 psi is installed in the line downstream of the main circulating pump. This switch has a high pressure and low pressure setting so that if system pressure is above or below these set values, the main pump is automatically shut off. All power to the test section and preheater is cut off automatically when the pump is shut off.

CHAPTER IV

CALIBRATION OF THERMOCOUPLES AND ORIFICE

Calibration of Thermocouples

A 30 gauge (.010-inch wire diameter) iron constantin thermocouple was made using wire from the same spool of thermocouple wire that was used to make all of the thermocouples used in the experiments. The thermocouple was attached to a terminal of the Brown temperature indicator and calibrated as the Brown indicator was used to measure all of the temperatures.

The thermocouple was calibrated by comparing the temperature indicated on the Brown indicator, with the freezing points of three metals, the boiling point of water, and the freezing point of water. Tin, lead, and zinc were chosen because their freezing points shown on Table I below, were in the temperature range over which the thermocouple was used.

TABLE I
FREEZING POINTS OF METAL SAMPLES

Metal	Freezing Point, F
Tin	449.42
Lead	621.32
Zinc	787.10

An electrically heated furnace, constructed for thermocouple calibration was used to melt each of the metal samples. The thermocouple used

in the calibration was inserted into a glass tube and the glass tube was inserted into the metal sample. Each metal sample was heated to a temperature of approximately 20 F above its melting point, and maintained at that temperature for ten minutes.

After the ten minute period, the power to the furnace was switched off and the sample was allowed to cool. While each of the samples cooled, the temperature indicated by the Brown indicator was recorded each minute. The cooling curves for the tin, lead, and zinc samples are shown on Figs. 8, 9, and 10, respectively. Each curve exhibits a characteristic undercooling time interval when the sample drops below the freezing point. The temperature then rises rapidly to the freezing point, and solidification proceeds in a normal manner as shown by the flat portion of each curve where the temperature remains constant over a period of minutes. This period is the freezing region. As shown on Figs. 8, 9, and 10, the freezing point indicated by the Brown indicator was 455 F, 627 F, and 792.5 F for the tin, lead, and zinc samples, respectively.

A comparison of these indicated freezing points was made with the known freezing points of the samples shown on Table I. The corrections to be applied to the indicated freezing points are shown on Table II.

TABLE II
TEMPERATURE CORRECTIONS DETERMINED FROM
FREEZING OF METAL SAMPLES

Indicated Temperature, F	Correction, F
455	- 5.58
627	- 5.68
792.5	- 5.40

These corrections for the various temperatures are plotted in Fig. 11.

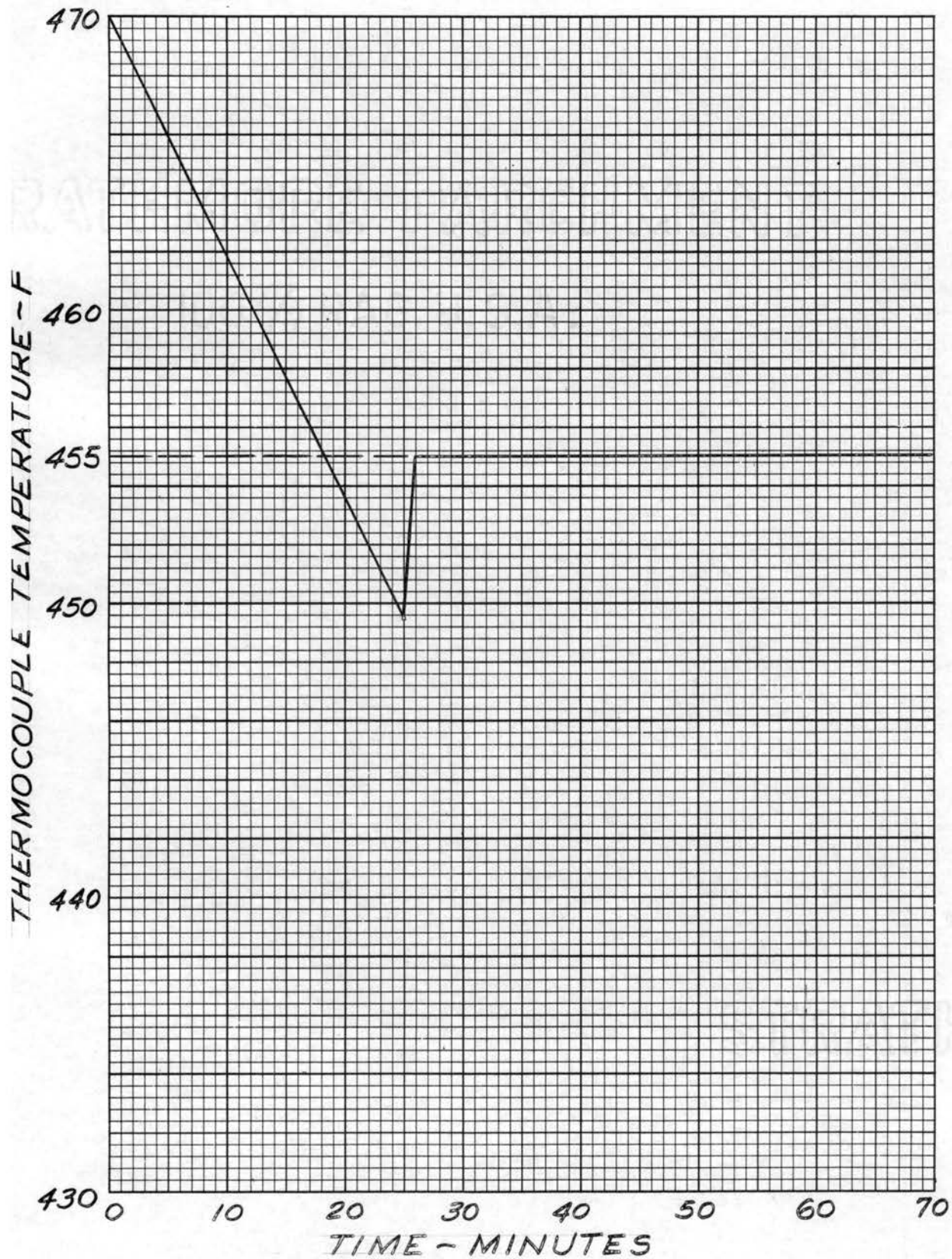


FIGURE 8
COOLING CURVE FOR TIN SAMPLE

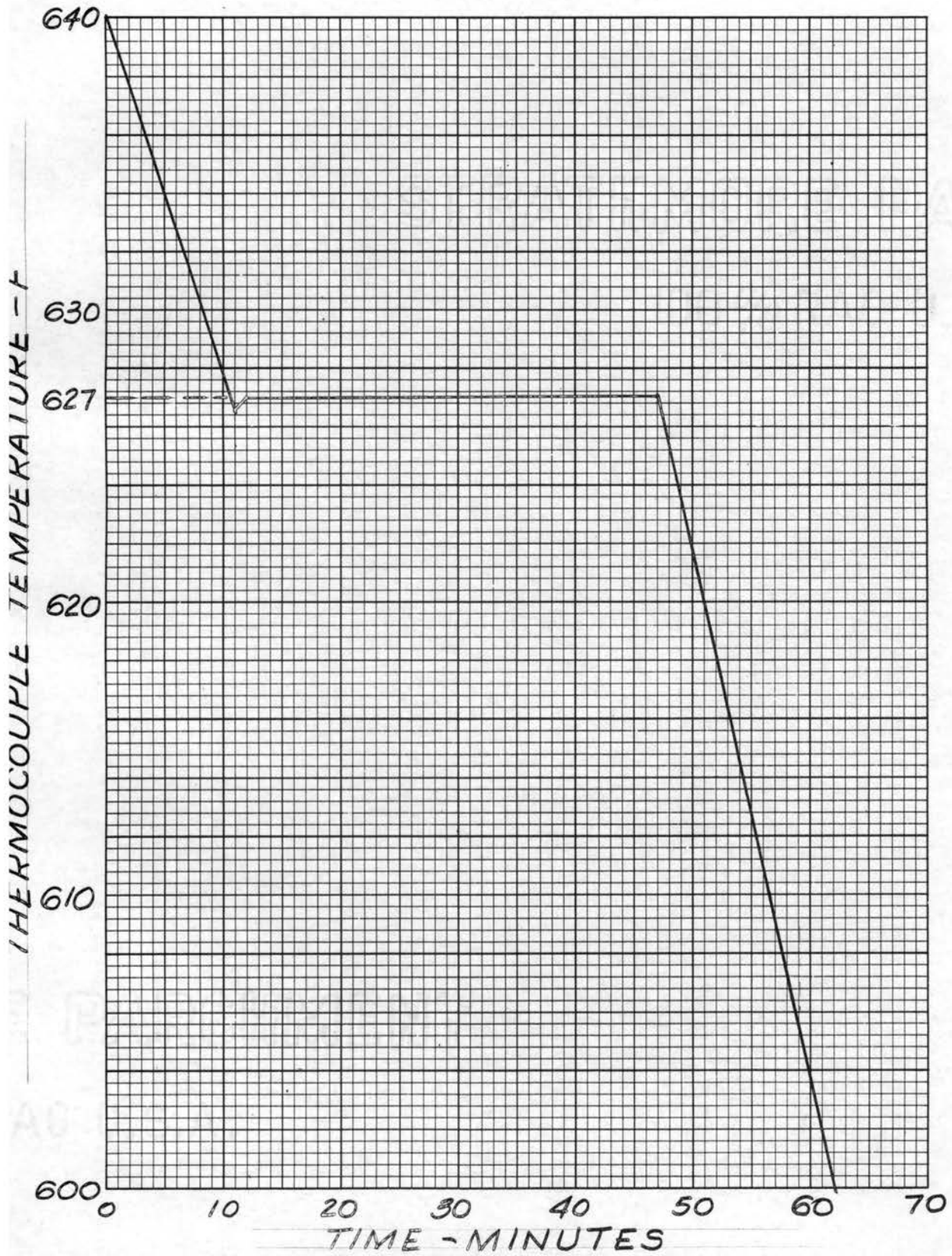


FIGURE 9

COOLING CURVE FOR LEAD SAMPLE

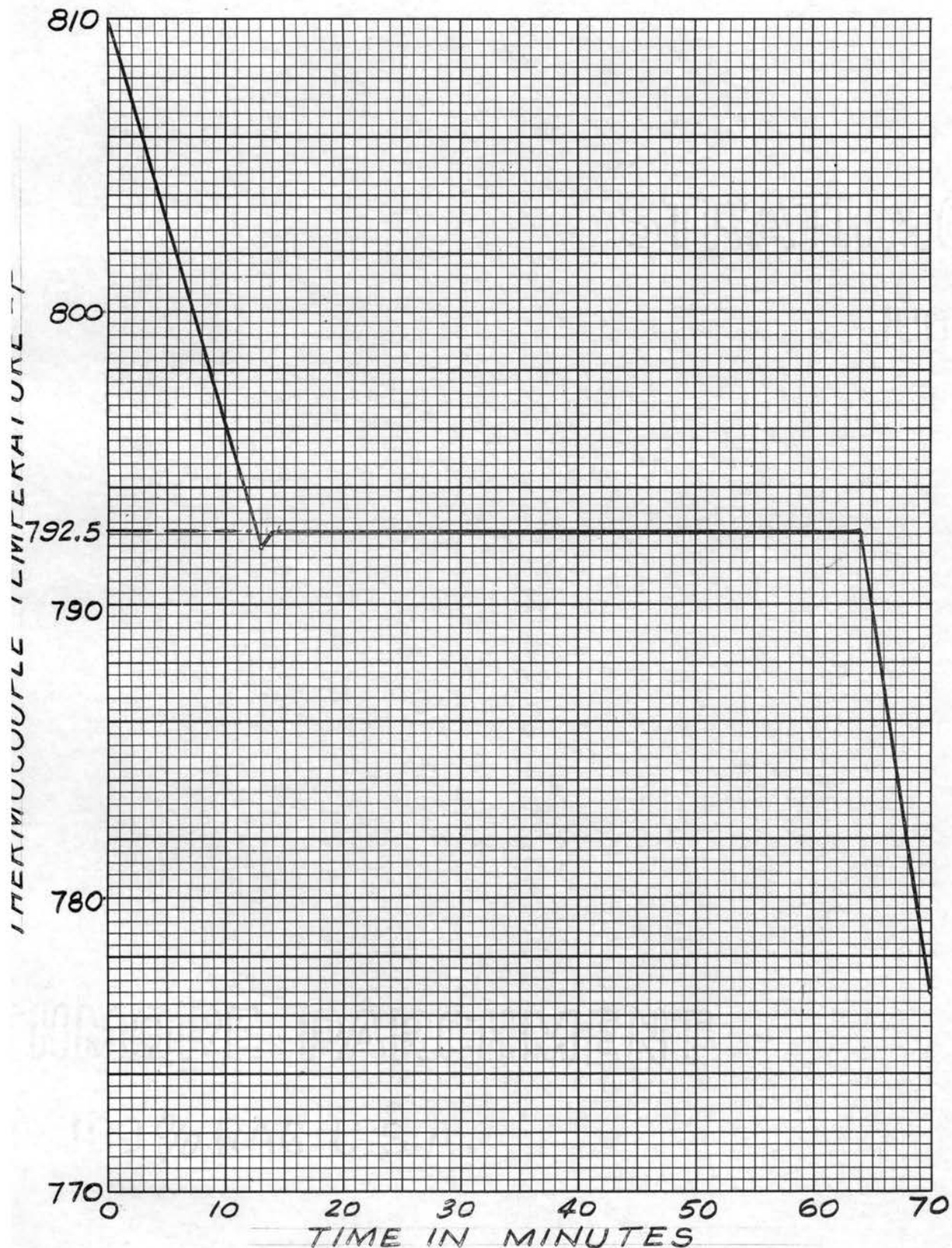


FIGURE 10
COOLING CURVE FOR ZINC SAMPLE

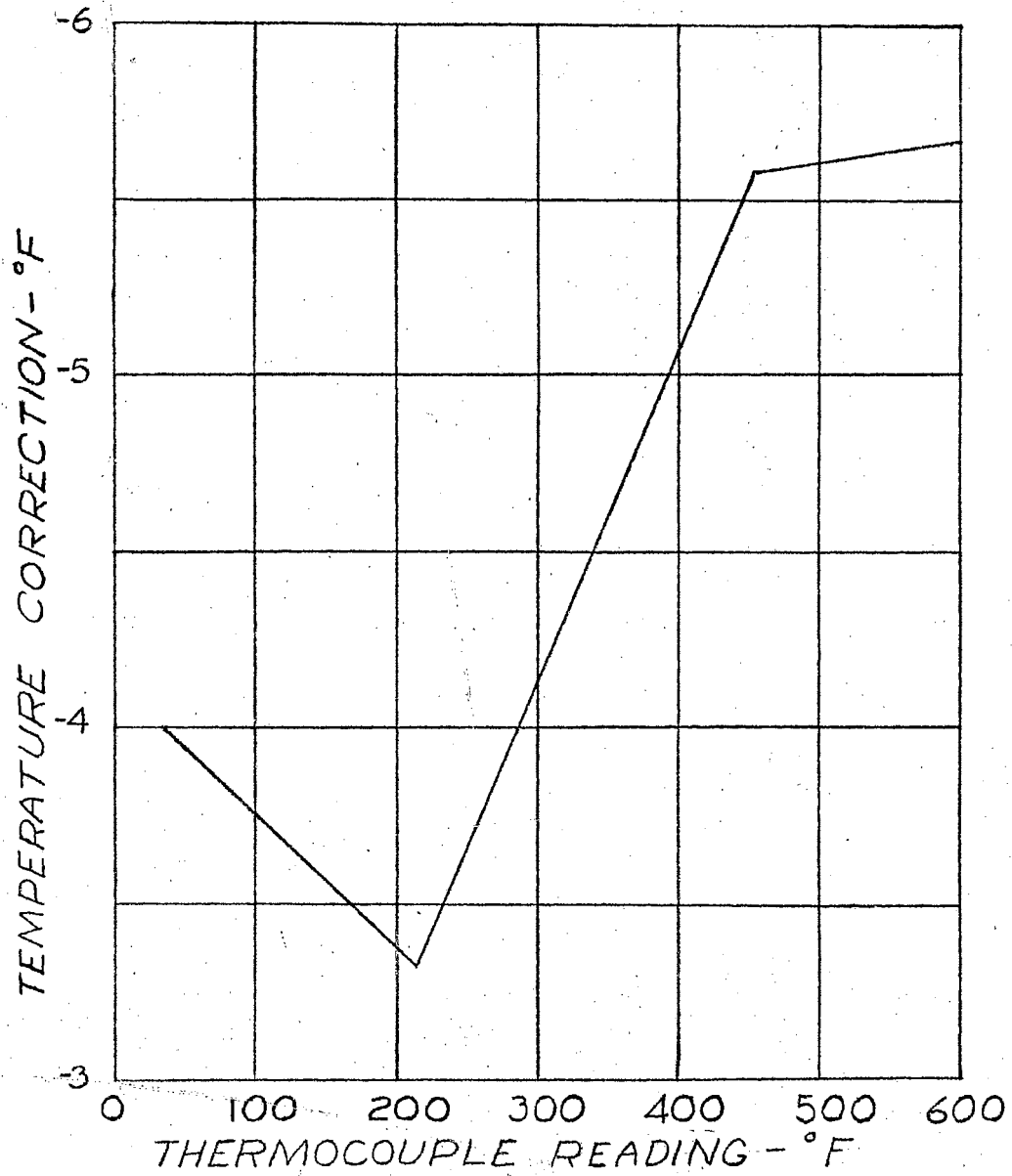


FIGURE- II
TEMPERATURE CORRECTION VS.
THERMOCOUPLE READING

To obtain the calibration data for the thermocouple at the boiling point of water, distilled water in a beaker was brought to boiling over an electric stove. The thermocouple was placed in the beaker, and was taped so that the junction of the thermocouple did not touch the side of the beaker. The Brown Electronik indicator temperature was 214 F. The barometric pressure reading was 29.165 inches of mercury. From Keenan and Keyes steam tables (5), the boiling point at this pressure was 210.68 F. Thus the thermocouple temperature, as indicated on the Brown indicator, was $214 - 210.68 = 3.32$ F too high for a reading of 215 F. This difference is plotted on Fig. 11, corresponding to a thermocouple reading of 214 F.

To obtain the calibration data for the thermocouple at the freezing point of water, a clean thermos bottle was filled with chipped frozen distilled water, and distilled water. The thermocouple was inserted in the thermos bottle and the ice-water mixture was thoroughly stirred. The Brown Electronik indicator reading was 36 F. Thus the thermocouple reading was 4 F higher than the freezing point of water, 32 F. This difference is plotted on the curve shown on Fig. 11, corresponding to a thermocouple reading of 32 F.

It was assumed that the temperature corrections for temperatures between the calibration points varied linearly with temperature. Thus adjacent calibration points were joined by a straight line, as shown on Fig. 11.

Calibration of .353-inch Diameter Orifice Plate

The basic equation relating volume rate of flow and manometer level, as used in orifice calibration work is :

$$V_1 = CA_c \sqrt{2gh_1} \quad , \quad \text{where} \quad (6)$$

V_1 = volume rate of flow, cubic feet per second

C = orifice coefficient of discharge

A_c = cross sectional area of internal pipe diameter, square feet

h_1 = differential head across orifice, in feet of fluid flowing

g = acceleration of gravity = 32.17 ft/sec².

The orifice was located in a 1-inch, schedule 40 pipe, having an internal diameter of 1.049 inch. The cross sectional area was then:

$$A_c = \pi(1.049)^2/4 (144) = .006005 \text{ ft}^2.$$

The flow rate was determined by weighing system fluid for a measured interval of time. The manometer system was bled to purge the lines of air at the appropriate places. It was difficult to remove all the air from the lines, and as a result some of the results were inconsistent: however, all the data used in the orifice coefficient calculations were taken with the manometer fluid returning to the $0 \pm .02$ mark after the main circulating pump was shut off.

The water flowing through the 0.353-inch orifice was directed into a container, and the system was allowed to reach a steady state. The system water was then diverted into a weighing tank situated on a platform scale. The water was diverted from the weighing tank after a minimum of three minutes. The weight of the water in the weighing tank was then measured. No corrections were necessary for the scales, as the maximum error in the range of the weights measured was 0.1 pound. A number of measurements were made at constant flow rate to check the consistency of the weighing. The maximum variation was 1/3%.

The data were taken to determine the value of the orifice coefficient under conditions of 50 psig pressure at the orifice plate, and temperatures

of from 70 to 83 F. The pressure was held constant to minimize the effect of any bubbles in the manometer sensing lines.

Figure 12 is a plot of $\log Re$ versus C . The Reynolds number, Re , was determined from the equation

$$Re = \frac{\rho v d}{\mu}$$

where the diameter of the orifice plate was used as the characteristic diameter, d . The temperature of the water upstream of the orifice was measured at each reading, and the Reynolds number adjusted accordingly. The value of the orifice coefficient, C , was determined from the basic equation

$$V_1 = CA_c \sqrt{2gh_1}$$

with the known values of V_1 and h_1 substituted. As shown on the figure, a straight line was found to represent the locus of these points with the maximum deviation from the line .0004 on the C axis, and the average about .0002. These deviations were 4/7 and 2/7% respectively.

Figure 13 is a log-log plot of the flow in lbs/min versus inches of manometer fluid (specific gravity 2.95). The plot was compared with the plot of Table 31 in the Flow Meter Engineering Handbook (6) for a standard sharp edged orifice. The two plots differed by 1% maximum.

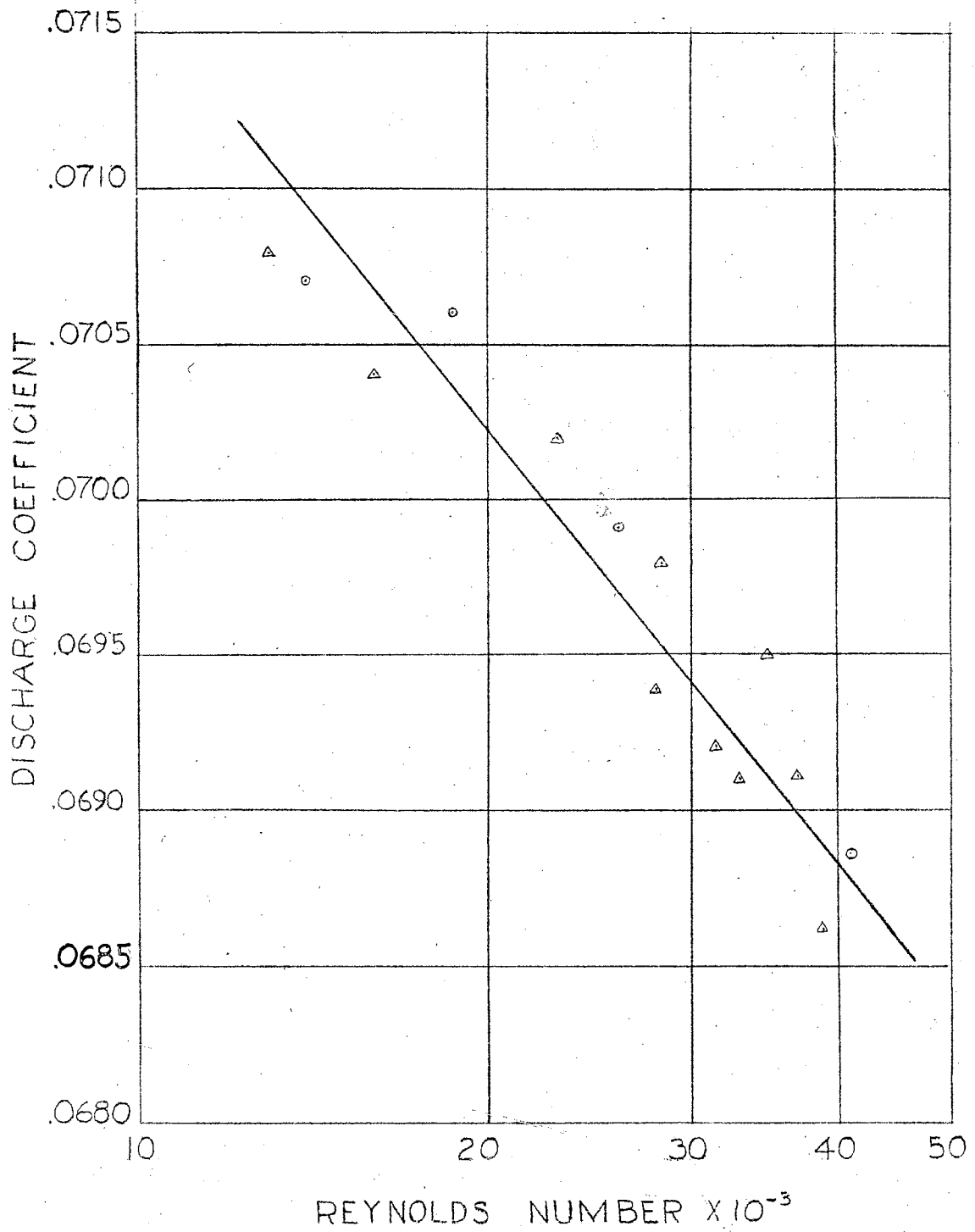
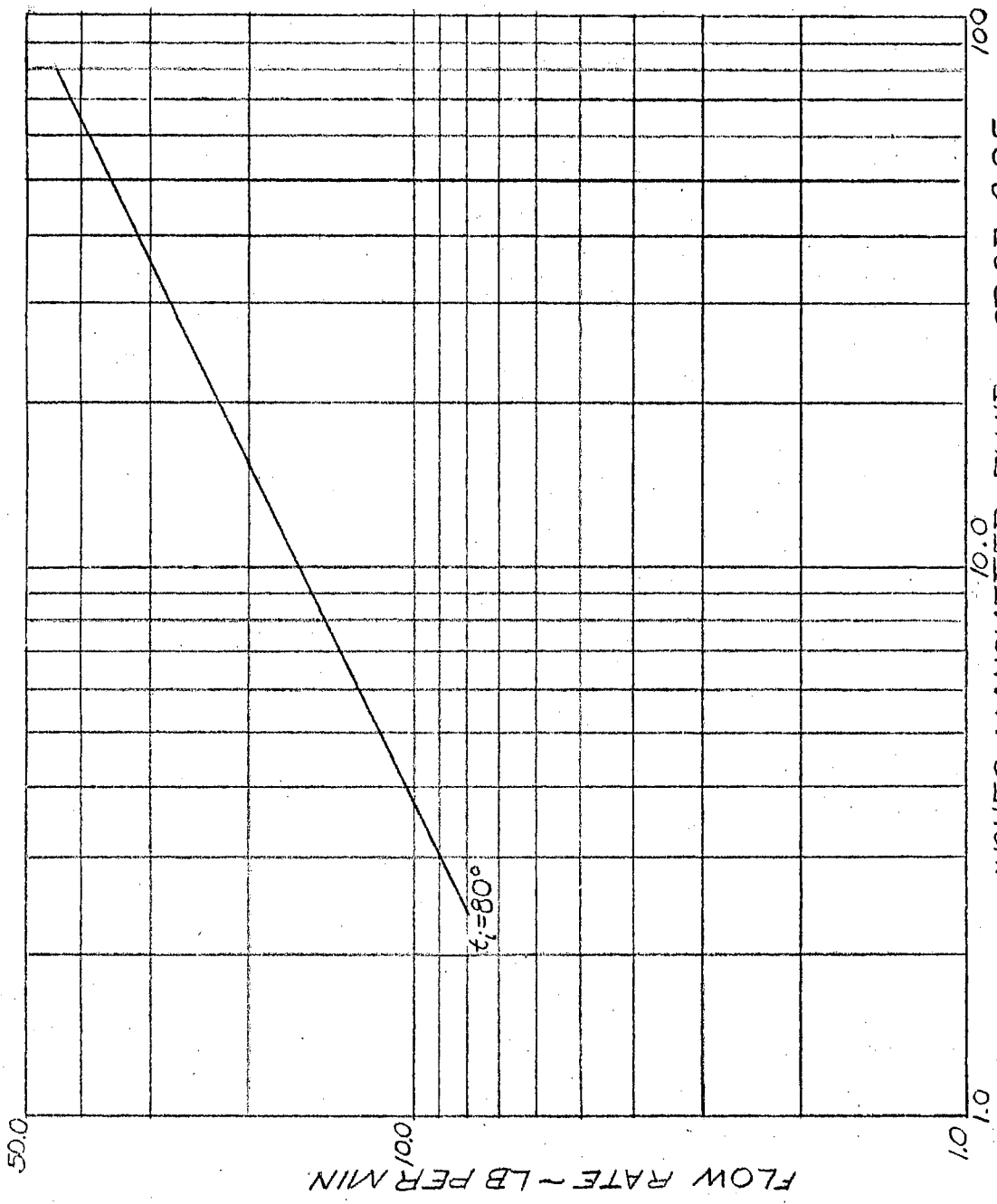


FIGURE-12
ORIFICE CALIBRATION CURVE



INCHES MANOMETER FLUID ~ SP. GR 2.95
FLOW RATE VS. IN. MANOMETER

FIGURE 13

CHAPTER V

EXPERIMENTAL PROCEDURE AND PRESENTATION OF DATA

Experimental Procedure

In order to operate the heat transfer loop, it was necessary to open the valves on the cooling water lines to the condenser and holdup tank as safety interlocks prevented application of power to the test section or the preheater. Also, the maximum allowable system pressure was set on the Murphy pressure switch.

Before any data were recorded, the manometers were bled to remove any air trapped in the manometer lines. The valves in the tops of the seal pots were opened at a test section pressure of from 10 to 30 psig, and the system fluid was allowed to bleed off until no air bubbles were present in the manometers.

At the beginning of each day of testing, manometer readings were taken without heat addition in the test section. These manometer readings were plotted versus distance along the test section, and a straight line was drawn through the locus of the points. If one of the manometer readings did not fall on the straight line, the scale of the manometer giving the incorrect reading was adjusted accordingly. The adjustments to the manometers were made under flow conditions since the meniscus of the manometer fluid was poorly defined under no flow conditions because of deposits inside the manometer glass.

During each run, the pump speed was held essentially constant while other parameters varied. The maximum flow rate through the test section was controlled by the needle valve in the exhaust manifold. Flow rates less than the maximum could be obtained by adjusting the bypass valve. The bypass valve allowed system water leaving the pump to bypass the test section and return to the holdup tank. In order to obtain a particular test section pressure and flow rate simultaneously, it was necessary to adjust both the needle valve and bypass valve several times. A change in the bypass valve setting, to obtain the desired flow rate, affected the system pressure; while a change in the needle valve setting, to obtain the desired system pressure, affected the flow rate.

Preheater power was adjusted to obtain the desired test section inlet temperature. For each combination of flow rate and system pressure several runs were made, each with a different test section inlet temperature. The run with the highest inlet temperature was made first and successive runs were made in order of decreasing test section inlet temperature. For each run, test section power was adjusted until a trace of bubbles was noted in the sight glass, indicating nucleate boiling in the test section. After the system had stabilized, the outside test section temperature and pressure profiles were recorded. Flow rate and pressure fluctuations were present at all times during recording of the data, requiring that one person make correcting adjustments continuously. Test section power, voltage drop, and current, as well as preheater current and voltage, were recorded for each run.

The holdup tank temperature was kept at 80 F to 90 F during the series of runs and was very stable during changes in test section and preheater power settings. The holdup tank cooling coils were not needed as the

condenser provided sufficient cooling.

A complete list of the data taken during each run is as follows:

1. Date
2. Observers
3. Barometric pressure
4. Ambient temperature
5. Pump speed, RPM
6. Holdup tank water temperature
7. Static pressure at entrance of test section
8. Flow manometer reading
9. Manometer readings at nine pressure taps along the test section
10. Voltage readings at five places along the test section
11. Powerstat current
12. Powerstat voltage
13. Direct connected current
14. Direct connected voltage
15. Test section wattage
16. Test section current
17. Orifice inlet temperature
18. Test section inlet temperature
19. Test section outlet temperature
20. Outside test section surface temperature at twenty six locations along the tube.

Presentation of Data

A total of 171 runs were made on the heat transfer loop at five flow rates; namely, 10.20, 12.22, 14.20, 16.18, and 18.19 lb/min. At each

flow rate tests were conducted at five system pressures (measured at the test section inlet); namely, 35, 85, 135, 185, and 235 psig. For each combination of flow rate and static pressure, test were conducted for from four to seven test section inlet temperatures.

Of the 171 runs, 30 were chosen for a heat transfer analysis of the film coefficient in the non-boiling region. The data for the 30 runs are presented in Table III. Only the data necessary to evaluate the film coefficient are included in the table. For example, pump speed, pressure drop, preheater power, and holdup water tank temperature data are not included.

Test section surface temperatures given in the table refer to the thermocouple number as shown in Fig. 5. Intermediate temperatures along the test section are not included as it was assumed in the analysis that the surface temperature of the midsection of any test increment was the average surface temperature for that increment for which the film coefficient was evaluated. In addition, surface temperatures are not included beyond thermocouple number 17 as in most runs local boiling occurred in the tube past this point.

TABLE III

TABULATION OF HEAT TRANSFER DATA

Run	System Pressure psig	P	Flow Manometer in. Red Fluid	Orifice Inlet Temp., F	t_e	l_7	t_{w7}	l_9
22	35	22.80	12.80	80	179	3.8125	286	9.8125
23	35	16.05	12.80	85	207	3.8125	280	9.8125
24	35	8.98	12.80	85	238	3.8125	275	9.8125
24	35	32.10	12.80	83	130	3.8125	292	9.8125
117	35	24.00	12.80	82.5	149.5	3.8125	268	9.8125
118	35	35.58	12.80	83	86	3.8125	287	9.8125
10	85	23.40	10.00	81.5	220	3.8125	330	9.8125
11	85	17.70	10.00	85.5	251	3.8125	331	9.8125
12	85	25.26	10.00	86	205.5	3.8125	331	9.8125
13	85	31.50	10.00	85.5	182	3.8125	337	9.8125
128	85	30.30	10.00	87	150	3.8125	304	9.8125
42	135	18.24	7.70	89	251	3.8125	346	9.8125
43	135	21.48	7.70	89.5	240	3.8125	347	9.8125
44	135	27.00	7.70	89.5	204	3.8125	344	9.8125
137	135	13.51	7.70	85	190	3.8125	262	9.8125
138	135	31.50	7.70	86	150	3.8125	323	9.8125
68	185	6.57	5.65	91.5	311	3.8125	341	9.8125
69	185	12.18	5.65	93	276	3.8125	338	9.8125
70	185	17.70	5.65	91.5	251.5	3.8125	341	9.8125
71	185	21.60	5.65	92	231.5	3.8125	344	9.8125
72	185	25.20	5.65	92	210.5	3.8125	345	9.8125
73	185	29.88	5.65	93	173.5	3.8125	345	9.8125
74	185	34.92	5.65	91.5	139	3.8125	349	9.8125
147	235	6.00	3.90	96	353.5	3.8125	386	9.8125
148	235	9.03	3.90	96	326.5	3.8125	375.5	9.8125
149	235	12.36	3.90	96	301	3.8125	368	9.8125
150	235	15.96	3.90	96	268	3.8125	358	9.8125
151	235	21.30	3.90	96	241	3.8125	364	9.8125
152	235	23.82	3.90	96	216	3.8125	363	9.8125
153	235	28.50	3.90	96	185.5	3.8125	363	9.8125

TABLE III (Continued)

Run	t_{w9}	l_{11}	t_{w11}	l_{13}	t_{w13}	l_{15}	t_{w15}	l_{17}	t_{w17}
22	394	15.8125	299	21.8125	305	27.8125	314	33.8125	320
23	286	15.8125	291	21.8125	296	27.8125	303	33.8125	307
24	279.5	15.8125	281	21.8125	284.5	27.8125	288	33.8125	291
25	300	15.8125	307.5	21.8125	314	27.8125	325.5	33.8125	334
117	275	15.8125	280	21.8125	286	27.8125	294	33.8125	300
118	295	15.8125	300	21.8125	303	27.8125	313	33.8125	320
10	339	15.8125	346	21.8125	355	27.8125	365	33.8125	372
11	339	15.8125	342	21.8125	350	27.8125	357	33.8125	362
12	342	15.8125	351	21.8125	360	27.8125	371	33.8125	379
13	350	15.8125	360	21.8125	370	27.8125	382	33.8125	390
128	314	15.8125	323	21.8125	330	27.8125	340	33.8125	349
42	354	15.8125	360	21.8125	368	27.8125	376	33.8125	383
43	356	15.8125	362	21.8125	370	27.8125	380	33.8125	388
44	356	15.8125	364	21.8125	374	27.8125	386	33.8125	395
137	268	15.8125	272	21.8125	276	27.8125	283	33.8125	288
138	334	15.8125	343	21.8125	350	27.8125	362	33.8125	374
68	346	15.8125	347	21.8125	350	27.8125	354	33.8125	356
69	344	15.8125	349	21.8125	354	27.8125	360	33.8125	364
70	349	15.8125	357	21.8125	363	27.8125	372	33.8125	377
71	355	15.8125	361	21.8125	369	27.8125	380	33.8125	387
72	356	15.8125	367	21.8125	374	27.8125	386	33.8125	395
73	358	15.8125	367	21.8125	375	27.8125	389	33.8125	399
74	361	15.8125	371	21.8125	379	27.8125	392	33.8125	402
147	390	15.8125	391	21.8125	395	27.8125	399.5	33.8125	402
148	382	15.8125	385	21.8125	389	27.8125	395	33.8125	398
149	376	15.8125	380	21.8125	387	27.8125	394	33.8125	400
150	369	15.8125	376	21.8125	381	27.8125	391	33.8125	398
151	377	15.8125	384	21.8125	392	27.8125	406	33.8125	416
152	375	15.8125	384	21.8125	391	27.8125	402	33.8125	414
153	377	15.8125	385	21.8125	394	27.8125	410	33.8125	422

CHAPTER VI

ANALYSIS OF DATA

Method of Analysis

The purpose of this analysis was to determine the film coefficients for heat transfer between the inside of the heated tube and the flowing water. The analysis will be restricted to that portion of the tube where forced convection existed. To simplify the analysis, heat transfer coefficients were evaluated at six points in the first three feet of the heated portion of the tube, since during the 30 runs investigated, local boiling always occurred downstream of this initial section.

A secondary object of the forced convection analysis was to compare the experimental data with the heat transfer coefficients evaluated using Colburn's equation. The film coefficient during forced convection has been correlated by Colburn (1) and expressed by dimensionless numbers in the equation

$$\frac{h_c D}{K} = 0.023 \left[\frac{GD}{\mu} \right]^{0.8} \left[\frac{\mu C_p}{K} \right]^n$$

where

$n = 0.3$ when the fluid is cooled

$n = 0.4$ when the fluid is heated

A plot of this equation, using $n = 0.4$, is shown in Fig. 14. The physical properties for water used in the equation were taken from the figures

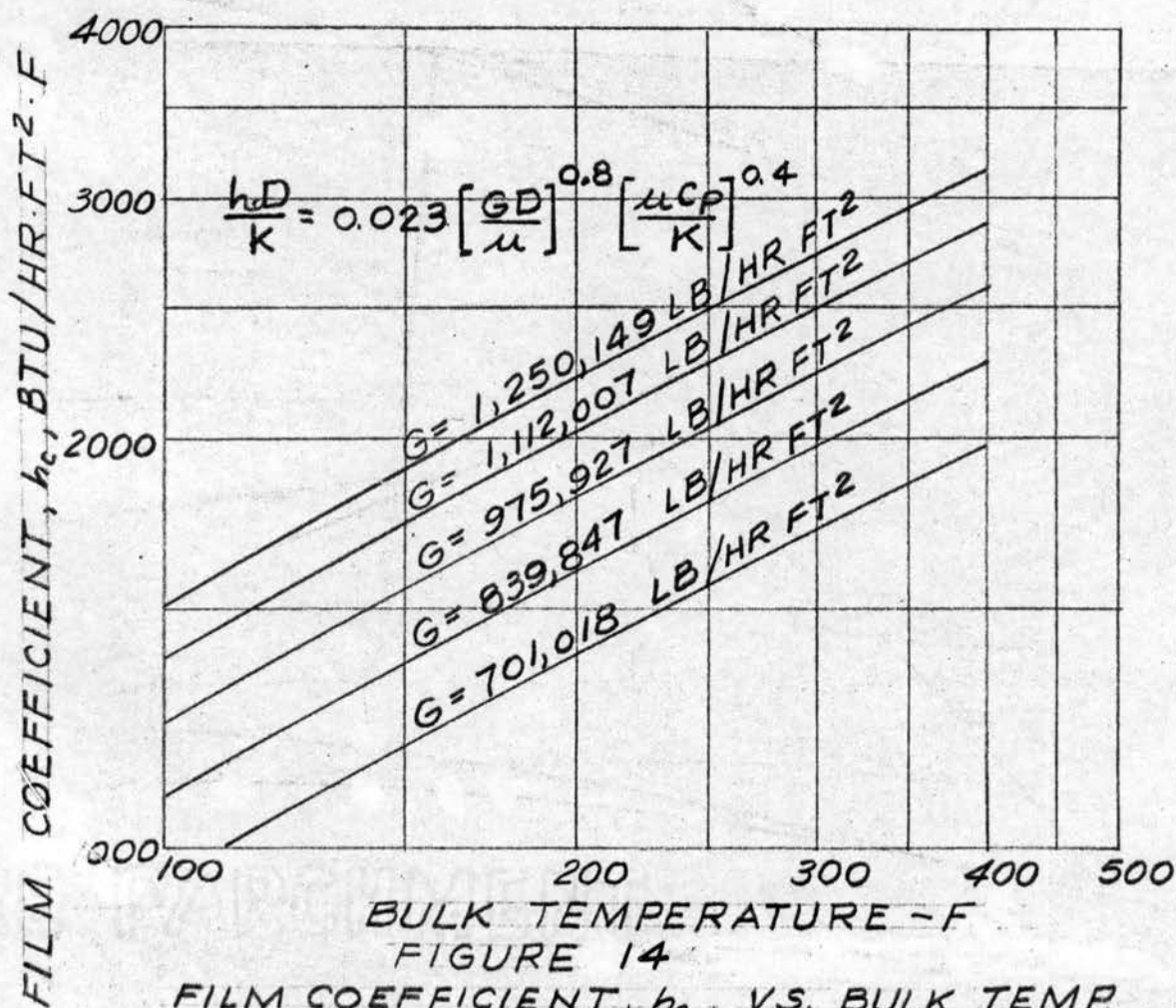


FIGURE 14
 FILM COEFFICIENT, h_c , VS. BULK TEMP.
 FOR HEATING WATER AT VARIOUS
 MASS FLOW RATES, G , INSIDE A
 TUBE WITH A .400 INCH I. D.

shown in the Appendix. Curves were plotted with the mass flow rate G as a parameter instead of bulk temperature since the film coefficients had to be determined at numerous bulk temperatures but at only five flow rates.

The following assumptions were made in the analysis:

1. Uniform heat generation
2. Uniform heat flux, along length
3. Steady state
4. Bulk temperature, considered to be thoroughly mixed fluid temperature at a cross section
5. Change in kinetic energy between the inlet and outlet of the test section, negligible
6. Fluid did no work
7. Average fluid properties used when calculating over a finite length of the tube
8. Unity power factor
9. Thermal expansion of the tube, negligible
10. Heat loss through insulation, heat loss along the axis of the tube, and heat loss from the power terminal lugs, negligible compared to the heat generation within the tube
11. The correction to flow rate for an orifice inlet temperature other than 80 F, negligible in this experiment, as deviation from 80 F was small

The voltage drops along the length of the tube are plotted in Fig. 15 for run number II. As shown in the figure, the voltage drop curve is a straight line. This means that the heat flux is uniform along the length of the tube, since the current must be constant at any cross-section.

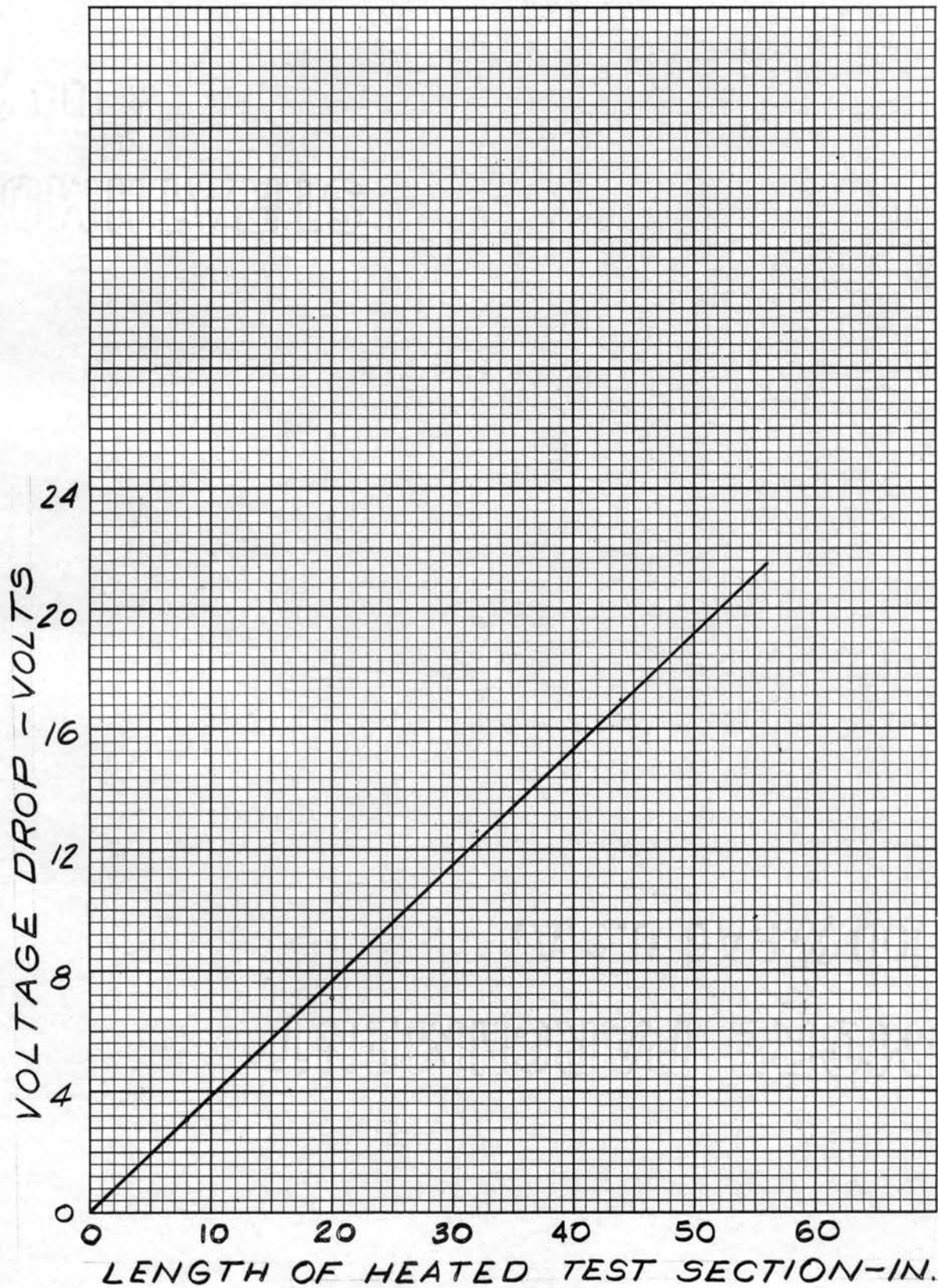


FIGURE 15

VOLTAGE DROP VS. LENGTH FOR RUN NO. 11

This curve is typical for all the runs investigated.

The following analysis for the heat loss through the insulation covering the test section demonstrates that the heat loss is negligible when compared to the heat generated in the tube.

The equation for the heat loss from a pipe covered with two layers of insulation was taken from Heat Transfer and Insulation by Jakob (7) and is

$$q' = \frac{2\pi (t_1 - t_3)}{\frac{\ln r_2/r_1}{K_{12}} + \frac{\ln r_3/r_2}{K_{23}}}$$

To be conservative, it was assumed that the entire length of the tube was at the highest temperature recorded along the tube. The highest test section wall temperature experienced during the thirty runs analyzed herein occurred on the tube during run number 153 and was 416.5 F. Similarly, the outside surface temperature of the insulation was the same as the room temperature. A low value of 80 F was chosen. The average values of the thermal conductivity of the asbestos and glass wool insulations are .117 and .03 Btu/hr F ft. respectively. These thermal conductivity values were estimated from data given in Handbook of Engineering Fundamentals by Eshbach (8).

The thickness of the asbestos was 1/16-inch, and the outside diameter of the glass wool insulation was 3 3/4-inch. Thus for a 1/2-inch diameter tube:

$$r_1 = 0.0417 \text{ ft}$$

$$r_2 = 0.0469 \text{ ft}$$

$$\text{and } r_3 = 0.1563 \text{ ft.}$$

The heat loss per foot is then:

$$\begin{aligned}
 q' &= \frac{2\pi(t_1 - t_3)}{\frac{\ln r_2/r_1}{K_{12}} + \frac{\ln r_3/r_2}{K_{23}}} \\
 &= \frac{2\pi(416.5 - 80)}{\frac{\ln 0.0469/0.0417}{0.117} + \frac{\ln 0.1563/0.0469}{0.03}} \\
 &= 51.57 \text{ Btu/hr ft}
 \end{aligned}$$

The heat flux generation rate for run number 153, was 20,844 Btu/hr ft. The heat loss through the insulation represented

$$\frac{51.57}{20,844} = .00247 \text{ or } .025\%$$

of the total heat generated in the tube. Thus the heat loss through the insulation was negligible compared to the total heat generation in the tube and was neglected in the heat transfer calculations.

The heat transfer coefficient was evaluated at 6-inch intervals in the first 3 feet of the heated portion of the tube. These points were conveniently chosen to coincide with thermocouple positions on the outer surface of the tube. Thermocouple positions 7, 9, 11, 13, 15, and 17 were used as the evaluation points. Thermocouple number 7 was 13/16-inch downstream from the inlet power terminal.

The heat balance equations for calculating the temperature rise during forced convection will be based on an average specific heat, \bar{C}_p . To avoid a reiteration process to determine Δt to a point, the average

specific heat was based on the average of the fluid temperature at the inlet of the test section and the temperature of the fluid at the preceding evaluation point. A plot of C_p versus temperature for water is shown in the Appendix. The equation for the temperature rise is:

$$\Delta t_{b_i} = \frac{P(3413)l_i}{60W\bar{C}_pL} = 1.0158 \frac{Pl_i}{W\bar{C}_p} .$$

The bulk temperature at any point in the forced convection portion of the tube is then:

$$t_{b_i} = t_e + \Delta t_{b_i}$$

The equation for the wall temperature drop is: (9)

$$t_{w_i} = \frac{-r_i q''}{24(r_o^2 - r_i^2)K} \left[(r_o^2 - r_i^2) - 2r_o^2 \ln \frac{r_o}{r_i} \right] .$$

with values of

$$r_o = .250\text{-inch}$$

$$r_i = .200\text{-inch}$$

and $K = 8.5(1 + .000517t_{w_i})$ for type 304 stainless steel, this equation becomes:

$$\Delta t_{w_i} = 2.344 \times 10^{-4} \frac{q''}{(1 + .000517t_{w_i})} .$$

A curve of K versus temperature for type 304 stainless steel is given in the Appendix.

The inside surface temperature of the tube can now be evaluated from:

$$t_{s_i} = t_{w_i} - \Delta t_{w_i} .$$

The determination of the film temperature drop can be accomplished by applying the following equation:

$$\Delta t_{f_i} = t_{s_i} - t_{b_i}$$

The heat transfer film coefficient can now be found from

$$\begin{aligned} h_i &= \frac{P(3413) \Delta 1}{A \Delta t_{f_i} L} = \frac{P(3413) \Delta 1}{\pi (.03334) \Delta 1 (L) \Delta t_{f_i}} \\ &= \frac{P(3413) (12)}{\pi (.03334) (56) (\Delta t_{f_i})} = 6982.48 \frac{P}{\Delta t_{f_i}} \end{aligned}$$

In order to compare the calculated film coefficient with the film coefficient from the Colburn equation, it was necessary to compute the mass flow rate. The mass flow rate, G , may be calculated from

$$G = \frac{60W}{A_s} = \frac{60W(4)}{\pi (.03334)^2} = 68,727.28W$$

The Colburn film coefficient may now be found from Fig. 14 using the bulk temperature of the fluid at the point of evaluation, t_{b_i} , and the mass flow rate, G , determined above.

The calculated film coefficient may be compared with the Colburn film coefficient, by using the simple ratio

$$h_i/h_{c_i} = \text{Calculated film Coefficient/Colburn film coefficient.}$$

The results of the evaluation of the heat transfer film coefficient for the 30 runs investigated are shown on Table IV. The inlet temperature of the fluid and the tube wall temperatures tabulated on Table IV have been corrected by applying the temperature correction of Fig. 11. The flow rate, W , was found from Fig. 13, using the flow manometer data of Table III.

TABLE IV
RESULTS OF HEAT TRANSFER ANALYSIS

Run	System Pressure psig	P	W	G	t_e	l_7	t_{w7}
22	35	22.80	18.19	1,250,149	175.7	3.8125	282
23	35	16.05	18.19	1,250,149	203.5	3.8125	276
24	35	8.98	18.19	1,250,149	234.5	3.8125	271
25	35	32.10	18.19	1,250,149	126.5	3.8125	288
117	35	24.00	18.19	1,250,149	146	3.8125	264
118	35	35.58	18.19	1,250,149	82	3.8125	283
10	85	23.40	16.18	1,112,007	216.5	3.8125	325.5
11	85	17.70	16.18	1,112,007	247.5	3.8125	326.5
12	85	25.26	16.18	1,112,007	202	3.8125	326.5
13	85	31.50	16.18	1,112,007	178.5	3.8125	332.5
128	85	30.30	16.18	1,112,007	146.5	3.8125	300
42	135	18.24	14.20	975,927	247.5	3.8125	341.5
43	135	21.48	14.20	975,927	236.5	3.8125	342.5
44	135	27.00	14.20	975,927	200.5	3.8125	339.5
137	135	13.51	14.20	975,927	186.5	3.8125	258
138	135	31.50	14.20	975,927	146.5	3.8125	318.5
68	185	6.57	12.22	839,847	307	3.8125	336.5
69	185	12.18	12.22	839,847	272	3.8125	333.5
70	185	17.70	12.22	839,847	248	3.8125	336.5
71	185	21.60	12.22	839,847	228	3.8125	339.5
72	185	25.20	12.22	839,847	207	3.8125	340.5
73	185	29.88	12.22	839,847	176	3.8125	340.5
74	185	34.92	12.22	839,847	135.5	3.8125	344.5
147	235	6.00	10.20	701,018	354	3.8125	381
148	235	9.03	10.20	701,018	322	3.8125	370.5
149	235	12.36	10.20	701,018	297	3.8125	363
150	235	15.96	10.20	701,018	264	3.8125	353.5
151	235	21.30	10.20	701,018	237.5	3.8125	359.5
152	235	23.82	10.20	701,018	212.5	3.8125	358.5
153	235	28.50	10.20	701,018	182	3.8125	358.5

TABLE IV (Continued)

Run	h_7	h_{c7}	h_7/h_{c7}	l_9	t_{w9}	h_9	h_{c9}
22	2305	2090	1.103	9.8125	290	2288	2130
23	2430	2240	1.085	9.8125	282	2394	2280
24	2890	2410	1.199	9.8125	275.5	2697	2420
25	2058	1770	1.163	9.8125	296	2108	1850
117	2139	1900	1.126	9.8125	271	2165	1560
118	1742	1500	1.161	9.8125	291	1790	1550
10	2312	2140	1.080	9.8125	334.5	2200	2180
11	2470	2280	1.083	9.8125	334.5	2397	2310
12	2122	2070	1.025	9.8125	337.5	2079	2110
13	2146	1940	1.106	9.8125	345.5	2117	2010
128	2048	1750	1.170	9.8125	310	2072	1820
42	1999	2040	.980	9.8125	349.5	1987	2080
43	2132	2000	1.066	9.8125	351.5	2132	2040
44	2004	1850	1.083	9.8125	351.5	1990	1900
137	1952	1760	1.109	9.8125	264	1941	1790
138	1846	1580	1.168	9.8125	329.5	1883	1650
68	2504	2040	1.227	9.8125	341.5	2274	2020
69	2089	1850	1.129	9.8125	335.5	2084	1920
70	2120	1820	1.164	9.8125	344.5	2143	1850
71	2020	1740	1.161	9.8125	350.5	2007	1780
72	1945	1660	1.172	9.8125	351.5	1973	1710
73	1839	1530	1.202	9.8125	353.5	1865	1600
74	1632	1350	1.209	9.8125	356.5	1691	1440
147	2518	1870	1.347	9.8125	385	2429	1880
148	1923	1790	1.074	9.8125	377	1848	1800
149	1944	1720	1.130	9.8125	371	1907	1740
150	1830	1620	1.119	9.8125	364	1777	1660
151	1758	1550	1.134	9.8125	372	1756	1590
152	1597	1460	1.094	9.8125	370	1636	1520
153	1575	1370	1.150	9.8125	372	1616	1420

TABLE IV (Continued)

Rum	h_9/h_{c9}	l_{11}	t_{w11}	h_{11}	h_{c11}	h_{11}/h_{c11}	l_{13}
22	1.074	15.8125	295	2375	2180	1.089	21.8125
23	1.050	15.8125	287	2408	2310	1.042	21.8125
24	1.114	15.8125	277	2877	2440	1.179	21.8125
25	1.139	15.8125	303.5	2172	1920	1.131	21.8125
117	1.105	15.8125	276	2251	2000	1.126	21.8125
118	1.155	15.8125	296	1882	1640	1.148	21.8125
10	1.055	15.8125	341.5	2352	2220	1.059	21.8125
11	1.038	15.8125	337.5	2574	2350	1.095	21.8125
12	.985	15.8125	346.5	2087	2150	.971	21.8125
13	1.053	15.8125	355.5	2150	2080	1.034	21.8125
128	1.138	15.8125	318.5	2130	1880	1.133	21.8125
42	.955	15.8125	355.5	2039	2100	.971	21.8125
43	1.045	15.8125	357.5	2227	2080	1.071	21.8125
44	1.047	15.8125	359.5	2063	1950	1.058	21.8125
137	1.084	15.8125	268	2014	1810	1.113	21.8125
138	1.141	15.8125	338.5	1955	1720	1.137	21.8125
68	1.126	15.8125	342.5	2550	2030	1.256	21.8125
69	1.085	15.8125	344.5	2131	1930	1.104	21.8125
70	1.158	15.8125	352.5	2165	1870	1.158	21.8125
71	1.128	15.8125	356.5	2137	1820	1.174	21.8125
72	1.154	15.8125	363.5	2002	1760	1.138	21.8125
73	1.166	15.8125	362.5	1965	1660	1.184	21.8125
74	1.174	15.8125	366	1786	1510	1.183	21.8125
147	1.292	15.8125	386	2821	1890	1.493	21.8125
148	1.027	15.8125	380	1973	1820	1.084	21.8125
149	1.096	15.8125	375	2047	1760	1.163	21.8125
150	1.070	15.8125	371	1844	1680	1.098	21.8125
151	1.104	15.8125	379	1876	1630	1.151	21.8125
152	1.076	15.8125	379	1720	1570	1.096	21.8125
153	1.138	15.8125	380	1740	1480	1.176	21.8125

TABLE IV (Continued)

Run	t_{w13}	h_{13}	h_{c13}	h_{13}/h_{c13}	l_{15}	t_{w15}	h_{15}
22	301	2430	2230	1.090	27.8125	309.5	2393
23	292	2423	2340	1.035	27.8125	299	2335
24	280.5	2808	2450	1.146	27.8125	284	2742
25	309.5	2274	2000	1.137	27.8125	321	2252
117	282	2318	2050	1.131	27.8125	290	2309
118	299	2018	1710	1.180	27.8125	309	2046
10	350.5	2340	2270	1.031	27.8125	360.5	2293
11	345.5	2494	2380	1.048	27.8125	352.5	2467
12	355.5	2094	2210	.948	27.8125	366	2063
13	365.5	2185	2130	1.026	27.8125	377	2186
128	325.5	2225	1950	1.141	27.8125	335.5	2253
42	363.5	2026	2140	.947	27.8125	371	2029
43	365	2277	2120	1.074	27.8125	375	2241
44	369	2105	2000	1.053	27.8125	381	2088
137	272	2091	1950	1.130	27.8125	279	2032
138	345.5	2065	1800	1.147	27.8125	357.5	2097
68	345.5	2571	2040	1.260	27.8125	349.5	2455
69	349.5	2180	1960	1.112	27.8125	355.5	2173
70	358.5	2269	1910	1.188	27.8125	367	2270
71	364.5	2216	1860	1.191	27.8125	375	2214
72	369	2145	1810	1.185	27.8125	381	2150
73	370	2107	1720	1.225	27.8125	384	2119
74	374	1915	1530	1.204	27.8125	387	1979
147	390	2760	1870	1.447	27.8125	394.5	2522
148	384	2046	1830	1.118	27.8125	390	1991
149	382	2051	1780	1.152	27.8125	389	2055
150	376	1980	1710	1.158	27.8125	386	1955
151	387	1986	1670	1.189	27.8125	401	1842
152	386	1853	1610	1.151	27.8125	397	1913
153	389	1867	1540	1.212	27.8125	405	1877

TABLE IV (Continued)

Run	h_{c15}	h_{15}/h_{c15}	l_{17}	t_{w17}	h_{17}	h_{c17}	h_{17}/h_{c17}
22	2270	1.054	33.8125	315.5	2448	2310	1.060
23	2360	.989	33.8125	303	2400	2390	1.004
24	2480	1.106	33.8125	287	2736	2480	1.103
25	2060	1.093	33.8125	329.5	2299	2130	1.079
117	2110	1.094	33.8125	296	2372	2160	1.098
118	1800	1.137	33.8125	315.5	2140	1890	1.132
10	2300	.997	33.8125	367	2361	2350	1.005
11	2400	1.028	33.8125	357.5	2542	2430	1.046
12	2250	.917	33.8125	374	2095	2300	.911
13	2190	.998	33.8125	385	2268	2250	1.008
128	2010	1.121	33.8125	344.5	2307	2080	1.109
42	2170	.935	33.8125	378	2048	2200	.931
43	2160	1.038	33.8125	383	2272	2180	1.042
44	2050	1.019	33.8125	390	2142	2100	1.020
137	1880	1.081	33.8125	284	2064	1900	1.086
138	1850	1.134	33.8125	369	2132	1920	1.110
68	2050	1.198	33.8125	351.5	2617	2060	1.270
69	1980	1.097	33.8125	359.5	2282	2000	1.141
70	1930	1.176	33.8125	372	2430	1970	1.234
71	1900	1.165	33.8125	382	2333	2150	1.065
72	1860	1.156	33.8125	350	2234	1900	1.176
73	1780	1.150	33.8125	394	2222	1830	1.214
74	1670	1.185	33.8125	397	2100	1700	1.207
147	1910	1.320	33.8125	397	2662	1920	1.386
148	1840	1.082	33.8125	393	2134	1860	1.147
149	1800	1.142	33.8125	395	2109	1820	1.159
150	1740	1.124	33.8125	393	2033	1770	1.149
151	1700	1.142	33.8125	411	1970	1740	1.132
152	1650	1.159	33.8125	409	1953	1690	1.156
153	1600	1.173	33.8125	416.5	1972	1650	1.195

Following is a sample calculation to demonstrate the calculation method.

Sample Calculation

The film coefficient was calculated for a position 9.8125-inches from the inlet power terminal for run number 11. This position corresponds to number 9 thermocouple.

The specific heat was evaluated at the average of the inlet temperature and the bulk fluid temperature at the preceding evaluation point. The temperature of the water at the inlet for this run was 247.5 F and the temperature at the preceding evaluation point, thermocouple position 7, was 251.68 F. Thus \bar{C}_p was evaluated at

$$\frac{t_e + t_{b7}}{2} = \frac{247.5 + 251.68}{2} = 250 \text{ F approximately.}$$

From Fig 17, \bar{C}_p is 1.0142 Btu/lb F. The flow rate, W, for this run was 16.18 lb/min. The length of the tube from the inlet power terminal to the point of evaluation, l_9 , is 9.8125-inches. The power input to the test section for run number 11 was 17.70 kw. The temperature rise of the fluid from the inlet to the point of evaluation was

$$\Delta t_{b9} = \frac{1.0158 P l_9}{W \bar{C}_p} = \frac{(1.0158)(17.70)(9.8125)}{(16.18)(1.0142)} = 10.75 \text{ F.}$$

The bulk temperature of the fluid at position 9 was

$$t_{b9} = t_e + \Delta t_{b9} = 247.5 + 10.75 = 258.25 \text{ F.}$$

The heat flux, q'' , for the inside surface of the tube was

$$q'' = 6,982.48 P = (6982.48)(17.70) = 123,590 \text{ Btu/hr ft}^2 .$$

The wall temperature of the tube at thermocouple position 9 was

$$t_{w9} = 334.5 \text{ F.}$$

The temperature drop across the tube wall was

$$\begin{aligned} \Delta t_{w9} &= 2.344 \times 10^{-4} \frac{q''}{(1 + .000517t_{w9})} \\ &= \frac{2.344 \times 10^{-4}(123,590)}{1 + (.000517)(334.5)} = 24.70 \text{ F.} \end{aligned}$$

The inside surface temperature was

$$t_{s9} = t_{w9} - \Delta t_{w9} = 334.5 - 24.70 = 309.80 \text{ F.}$$

The temperature drop across the film was

$$\Delta t_{f9} = t_{s9} - t_{b9} = 309.80 - 258.25 = 51.55 \text{ F.}$$

The film coefficient at thermocouple position 9 was

$$\begin{aligned} h_9 &= 6982.48 \frac{P}{\Delta t_{f9}} = \frac{(6982.48)(17.70)}{51.55} \\ &= 2397 \text{ Btu/hr ft}^2 \text{ F.} \end{aligned}$$

The mass flow rate for run number 11 was

$$G = 68,727.28W = (68,727.28)(16.18) = 1,112,007 \text{ lb/hr ft}^2.$$

Using the mass flow rate, G , and the bulk temperature of the fluid, t_{b9} , the Colburn film coefficient was determined from Fig. 14.

$$h_{c9} = 2,310 \text{ Btu/hr ft}^2 \text{ F}$$

The ratio of the calculated film coefficient, h_9 , and the Colburn film coefficient, h_{c9} , was

$$h_9/h_{c9} = 2,397/2,310 = 1.038.$$

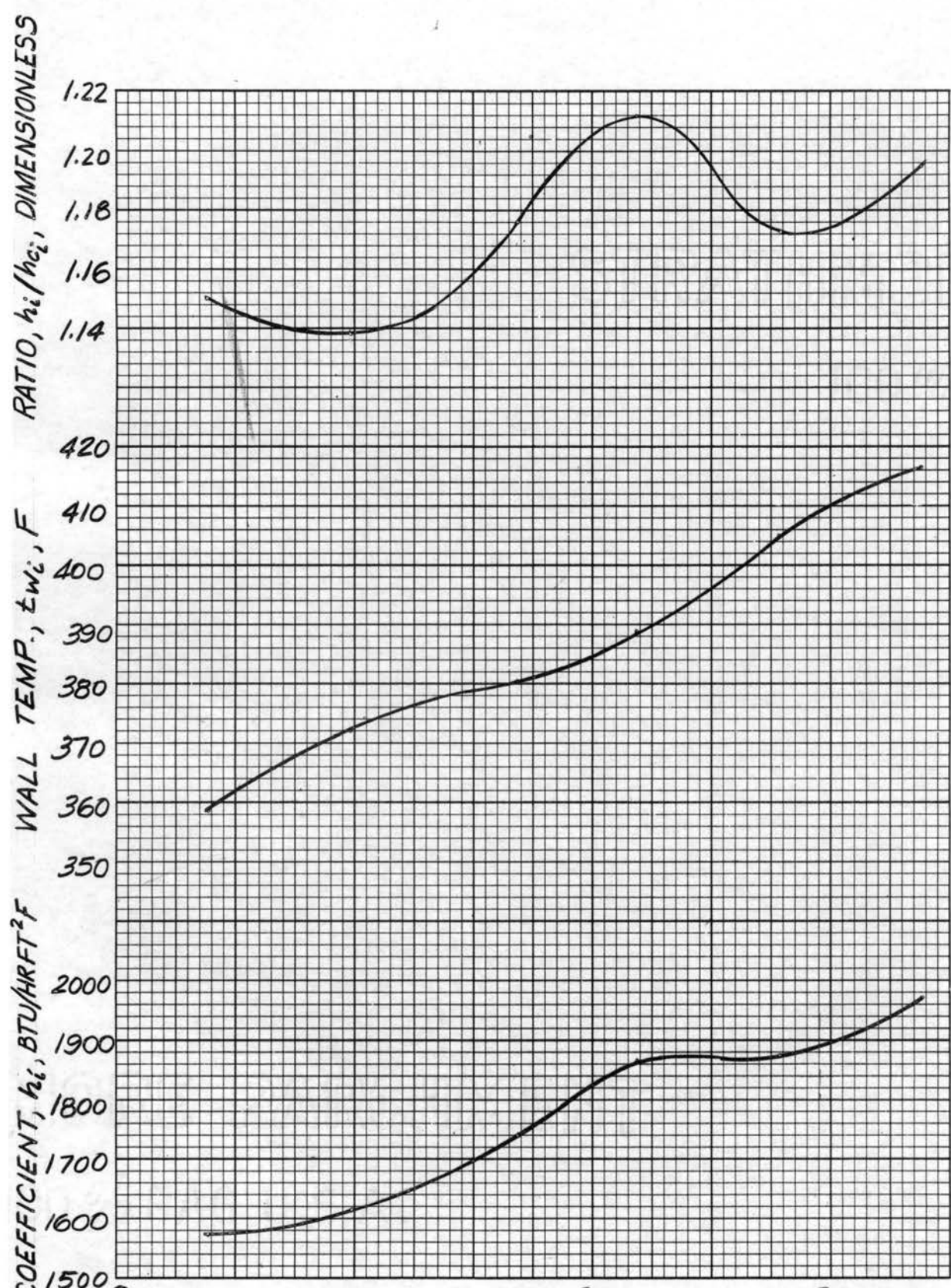
Thus the calculated film coefficient was 3.8% higher than that determined from the Colburn equation.

Discussion

The calculated film coefficients, the ratio of the calculated film coefficient to the film coefficients determined from the Colburn equation, and the outside surface temperature of the tube are plotted versus heated length of the test section for run number 153 in Fig. 16. This figure is typical for the other runs conducted. The ratio of calculated film coefficient to Colburn film coefficient varied from .98 to 1.493 although most of the ratios exceeded unity by a small amount. The highest ratios occurred during run number 147 where the power input was only 6.0 kw. It was reasoned that the wattmeter reading for this run was in error. The average ratio for all the film coefficients evaluated was approximately 1.11. Thus for the 30 runs evaluated, the calculated film coefficient was 11% higher than the film coefficient determined from the Colburn equation.

Upon comparing the results of the analysis shown on Table IV, the following conclusions can be stated.

1. Static pressure had little effect upon the film coefficient.
2. The heat transfer film coefficient increased with increasing bulk temperature.
3. The heat transfer film coefficient increased with increasing flow rate.



LENGTH OF HEATED TEST SECTION ~IN.

FIGURE 16

ANALYSIS RESULTS FOR RUN NO. 153

CHAPTER VII

CONCLUSIONS

It was found that the heat transfer coefficient increased with increasing mass flow rate and bulk temperature. Thus the film coefficient increased with length of heated section as the bulk temperature increased. Static pressure appeared to have little effect upon the value of the film coefficient.

For the 30 runs investigated, it was found that the heat transfer coefficients averaged 11% higher than those obtained from the Colburn equation. Because of the good agreement between the results of this experiment and those of the accepted semi-empirical Colburn equation, it is postulated that the heat transfer loop is adequate for future heat transfer experiments involving forced convection.

SELECTED BIBLIOGRAPHY

1. Colburn, A. P., "Method of Correlating Forced Convection Heat Transfer Data and A Comparison with Fluid Friction," Transactions of the American Institute of Chemical Engineers, 19, (1933).
2. Dittus, F. W., and Boelter, L. M. K., University of California Publication in Engineering, 2, 443, (1930).
3. Sieder, E. N., and Tate, G. E., Ind. Eng. Chem., 28, 1429-36, (1936).
4. Carpender, F. G., Colburn, P., Schoenborn, E. M., and Wurster, A., Trans. A.I. Ch. E., 29, 174-210, (1947).
5. Keenan, J. H., and Keyes, F. G., "Thermodynamic Properties of Steam," New York: John Wiley and Sons, (1936)..
6. "Flow Meter Engineering Handbook," Brown Instrument Co., (1936).
7. Jacob, M. and Hawkins, G. A., "Elements of Heat Transfer and Insulation". New York: John Wiley and Sons, 1950. Volume I, Second Edition.
8. Eshbach, O. W., "Handbook of Engineering Fundamentals". New York: John Wiley and Sons, Second Edition, (1952).
9. Rohde, R. R., "The Methods and Apparatus Used in the Experimental Determination of Water Film Coefficients". Argonne National Laboratory, Lemont, Illinois.

APPENDIX

PHYSICAL PROPERTIES OF WATER AND TYPE 304
STAINLESS STEEL

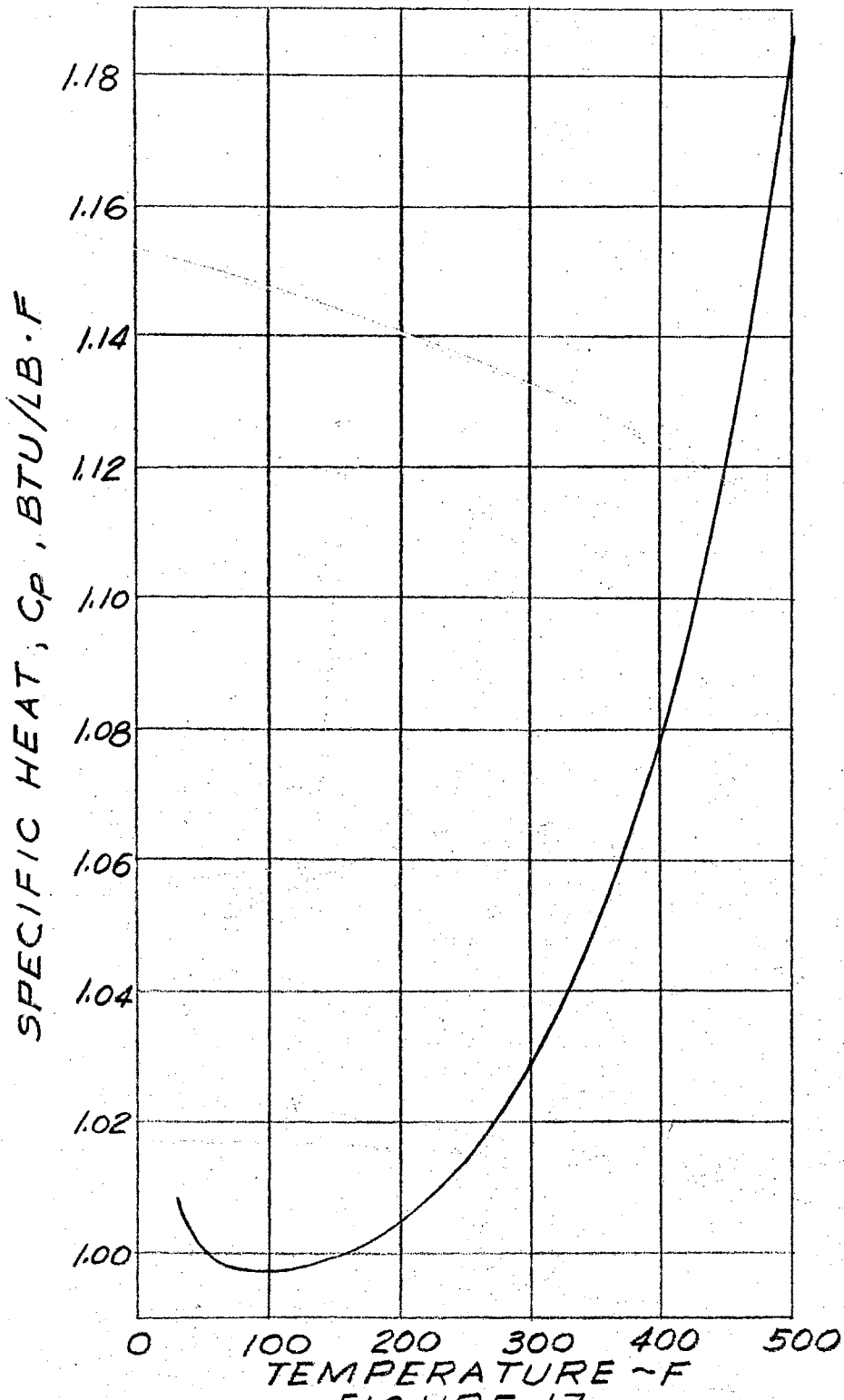


FIGURE 17
SPECIFIC HEAT VS TEMPERATURE
SATURATED LIQUID WATER

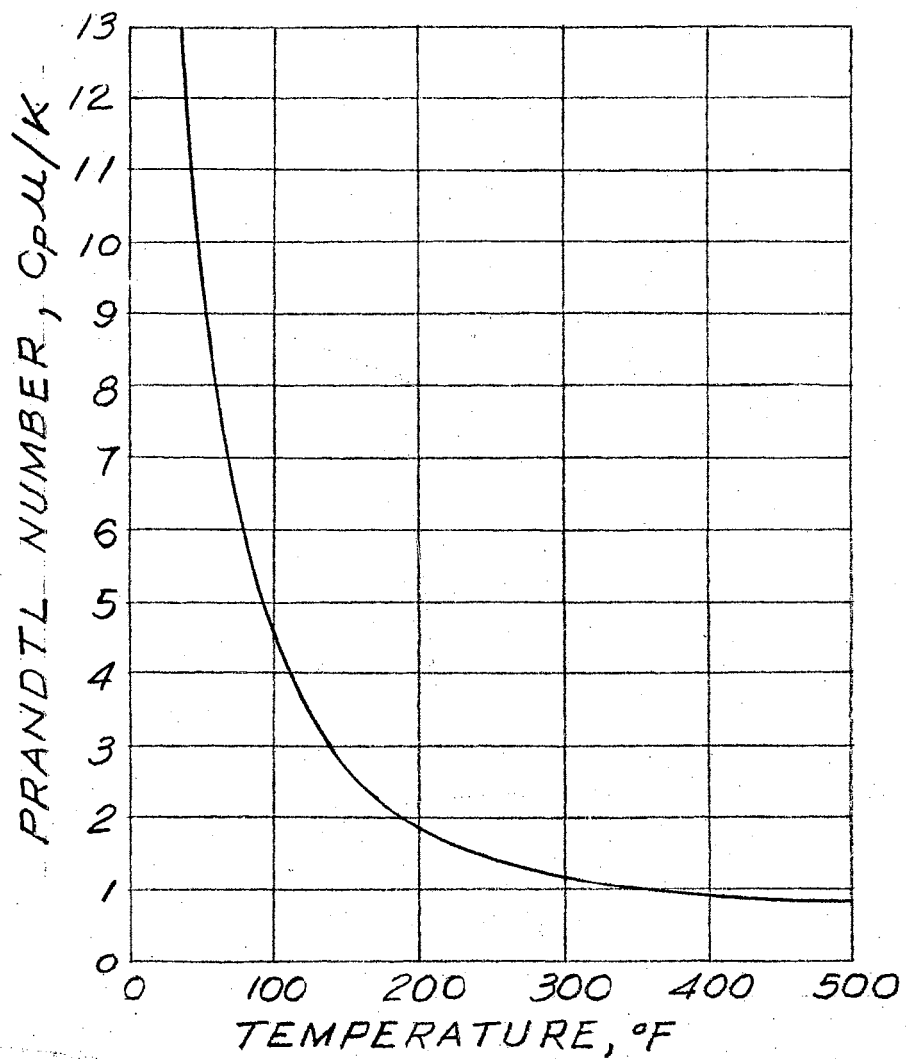


FIGURE 18
PRANDTL NUMBER VS. TEMPERATURE
SATURATED LIQUID WATER

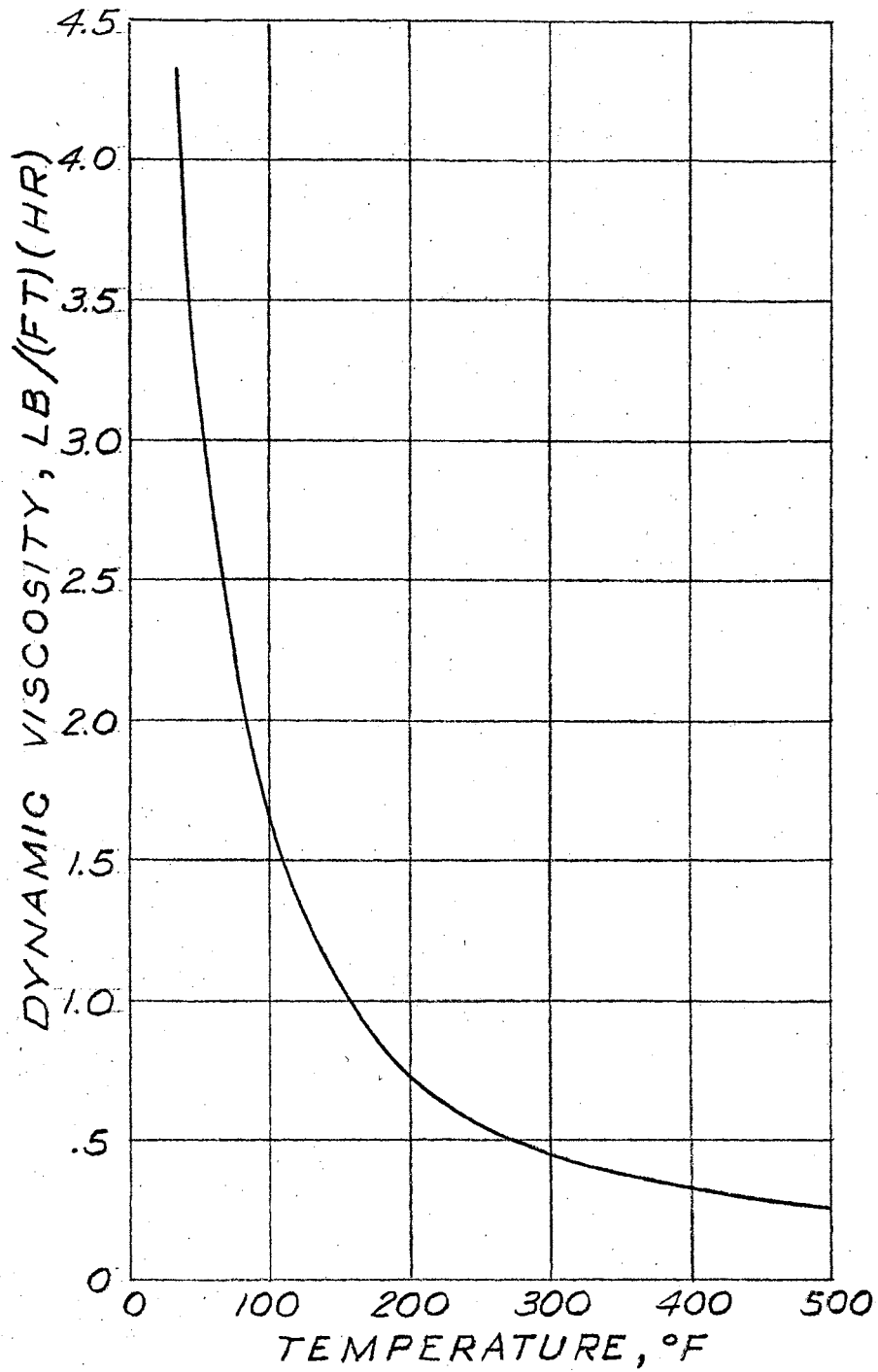


FIGURE 19
DYNAMIC VISCOSITY VS. TEMPERATURE
SATURATED LIQUID WATER

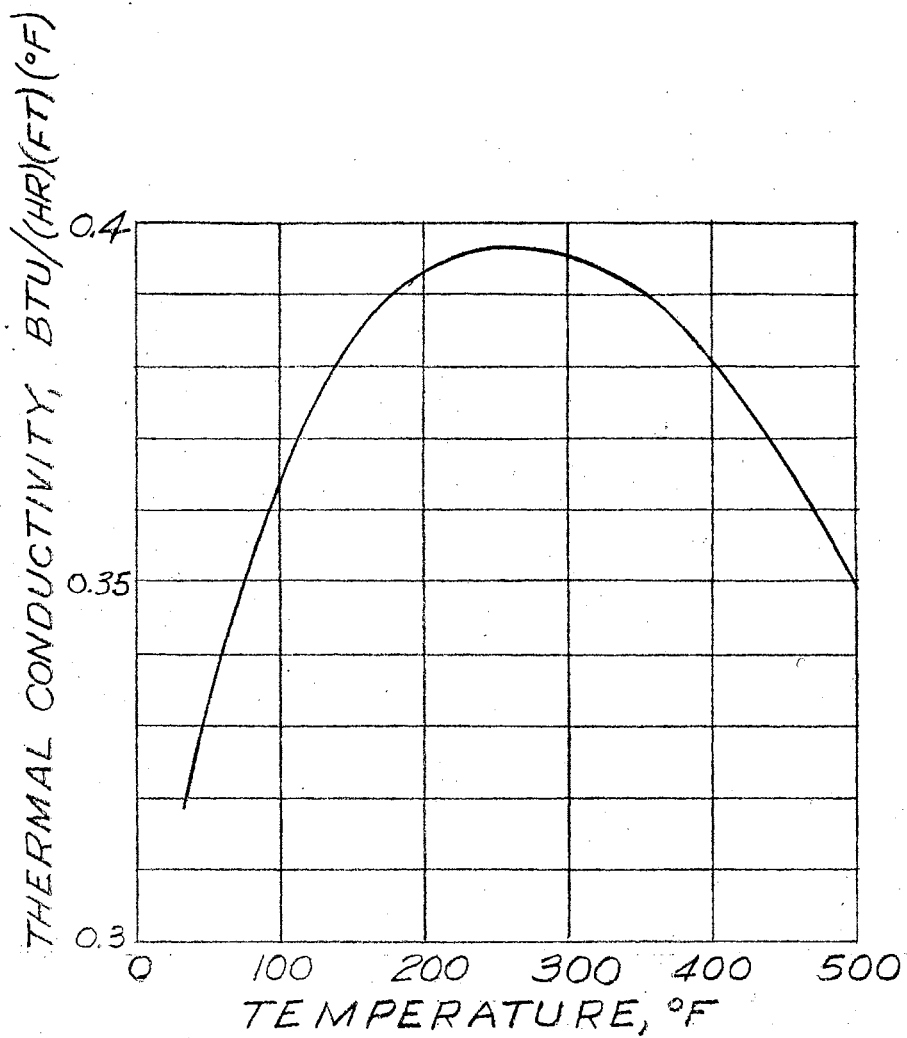


FIGURE 20
THERMAL CONDUCTIVITY VS.
TEMPERATURE FOR SATURATED
LIQUID WATER

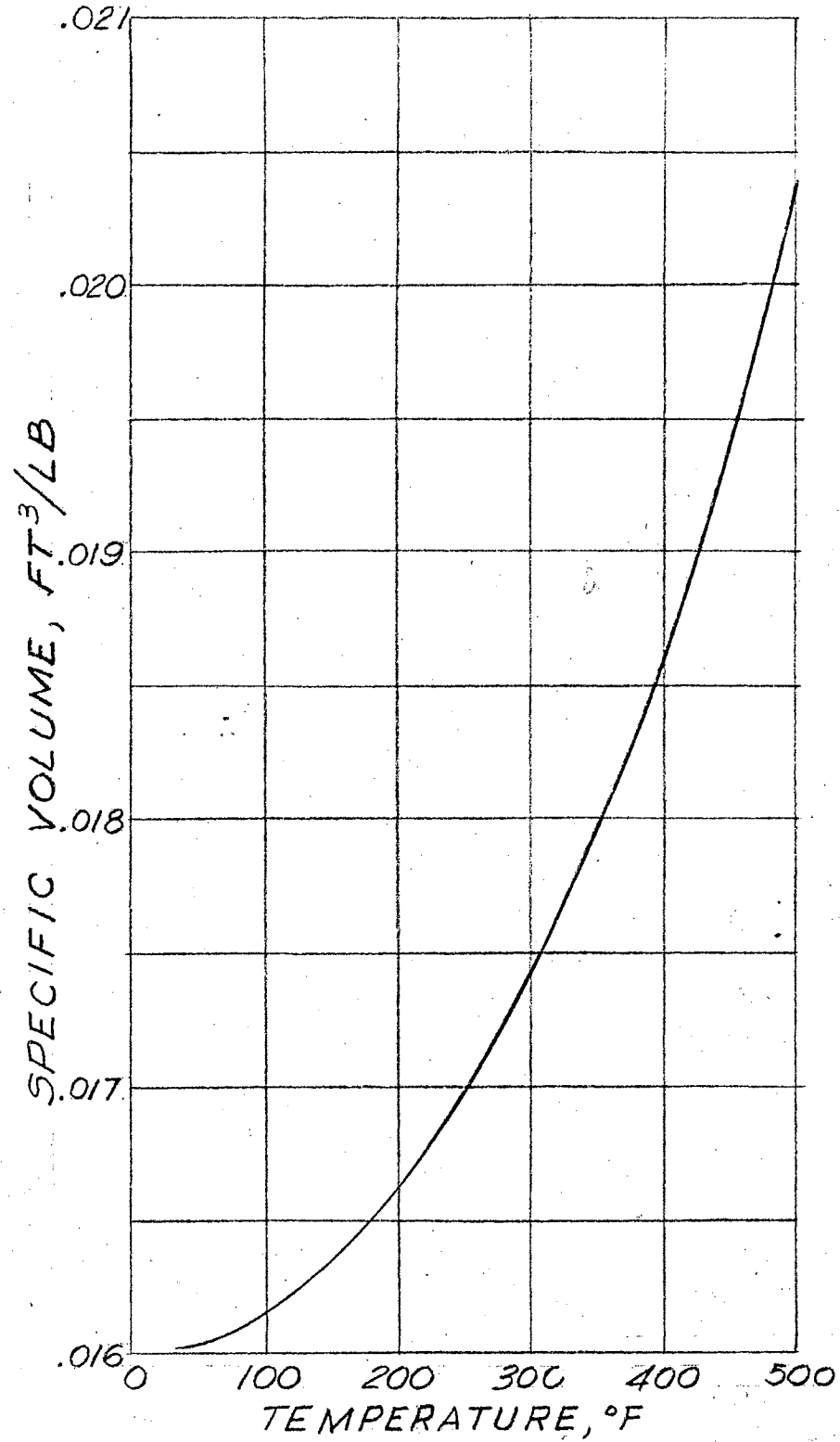


FIGURE 21

SPECIFIC VOLUME VS. TEMPERATURE SATURATED WATER

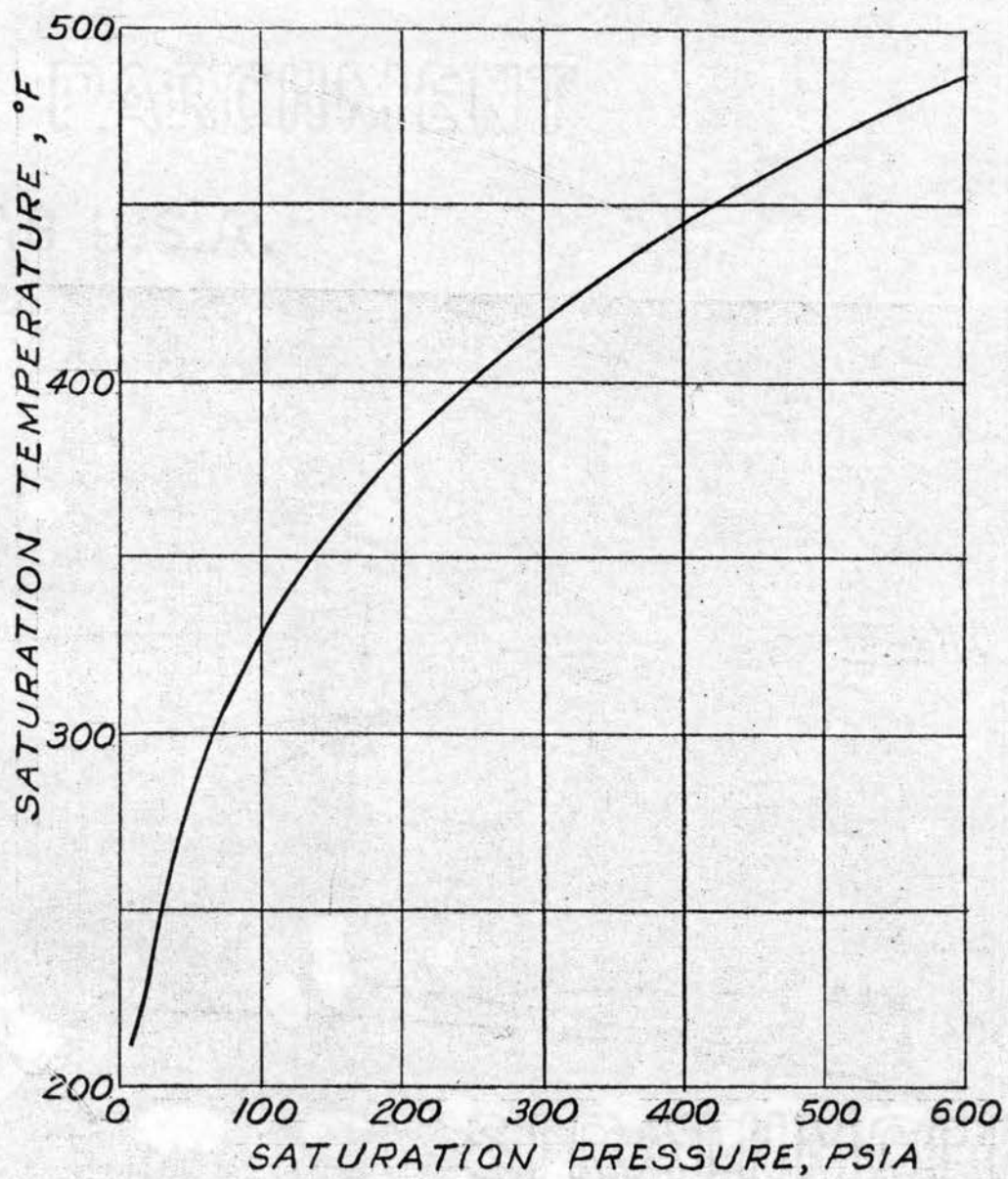


FIGURE 22
SATURATION TEMPERATURE V.S.
SATURATION PRESSURE FOR WATER

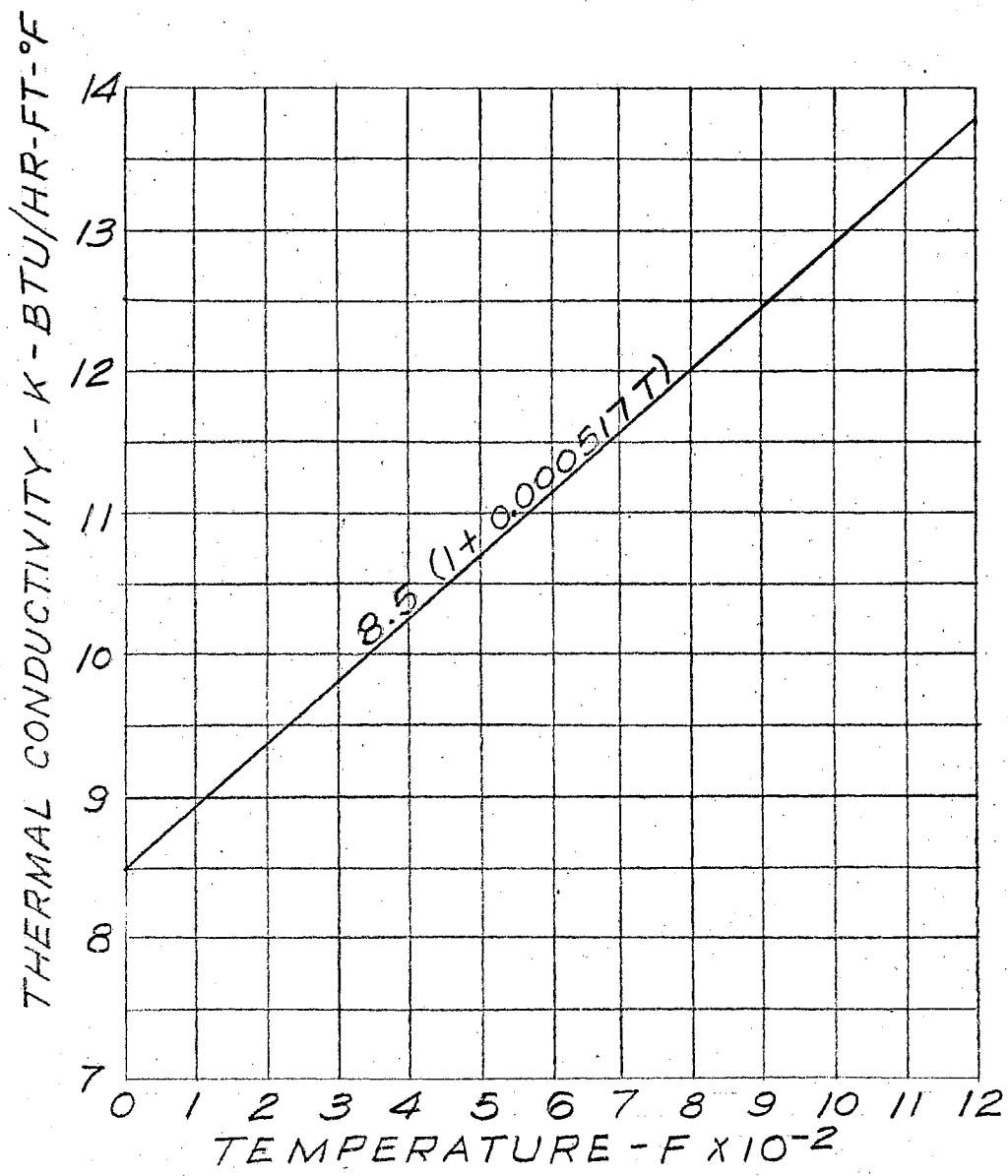


FIGURE 23
THERMAL CONDUCTIVITY
OF AISI TYPE 304
STAINLESS STEEL

VITA

Ross Siddons Philips

Candidate for the Degree of

Master of Science

Thesis: HEAT TRANSFER TO WATER FLOWING IN AN ELECTRICALLY HEATED
HORIZONTAL TUBE

Major Field: Mechanical Engineering

Biographical:

Personal data: Born at Oklahoma City, Oklahoma, July 1, 1926,
the son of James H. and Mabel A. Philips.

Education: Attended the Parker Vocational Cooperative High School
in Dayton, Ohio; entered the University of Oklahoma in
September, 1946 and received the Bachelor of Science
Degree in Mechanical Engineering in August, 1950; com-
pleted the requirements for the Master of Science degree
in May, 1959.

Experience: Worked as a tool designer while attending high school;
served in the U.S. Navy as a radar operator from December,
1944 until July, 1946; worked as an engineering designer
for the Douglas Aircraft Company, Northrop Aircraft Cor-
poration, Tempco Aircraft Corporation, Kaiser Metal
Products, and the Trane Company variously from August,
1950 until November, 1954; employed as a research engineer
by the Boeing Airplane Company since November, 1954.

Engineering fraternities: Member of Sigma Tau, Tau Beta Pi, Pi Tau
Sigma, and Tau Omega.